The Quark Anomalous Chromomagnetic Moment induced by QCD vacuum, a New Model for Pomeron and Odderon and Nonperturbative Quark Energy Loss in Quark-Gluon Matter

Nikolai Kochelev

BLTP, JINR, Dubna

CONTENTS

- Instantons
- Quark-quark and quark-gluon interactions induced by instantons
- Spin-spin quark interaction induced by Anomalous Quark Chromomagnetic Moment (AQCM)
- Soft Contribution to Quark-Quark Scattering coming from AQCM
- Pomeron structure
- Odderon structure and large $-t$ elastic hadron-hadron scattering
- Non-factorizable contribution to inclusive meson production
- Single-spin asymmetries in high energy reactions
- Non-perturbative energy loss by fast parton in strongly interacted Quark-Gluon Plasma (sQGP)

Instantons

QCD vacuum is not an empty space. There are strong topological fluctuations of gluon fields called instantons.
Chromomagnetic and Chromoelectric fields
$(\vec{E}^a)^2,\ (\vec{B}^a)^2 \neq 0$
in the QCD vacuum .

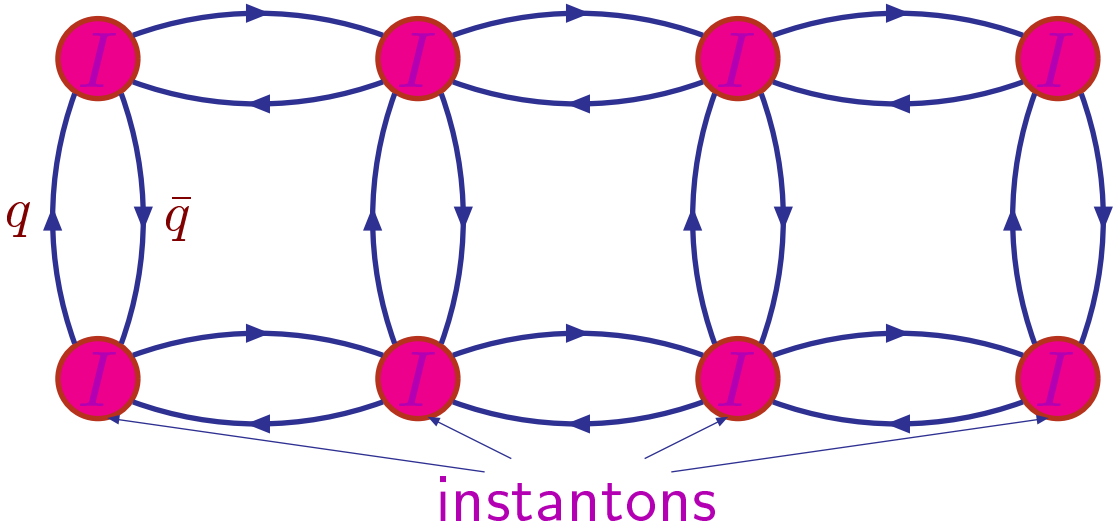

QCD vacuum structure is nontrivial: it is filled with instantons; quarks jump between them.

Analogy with the solid state

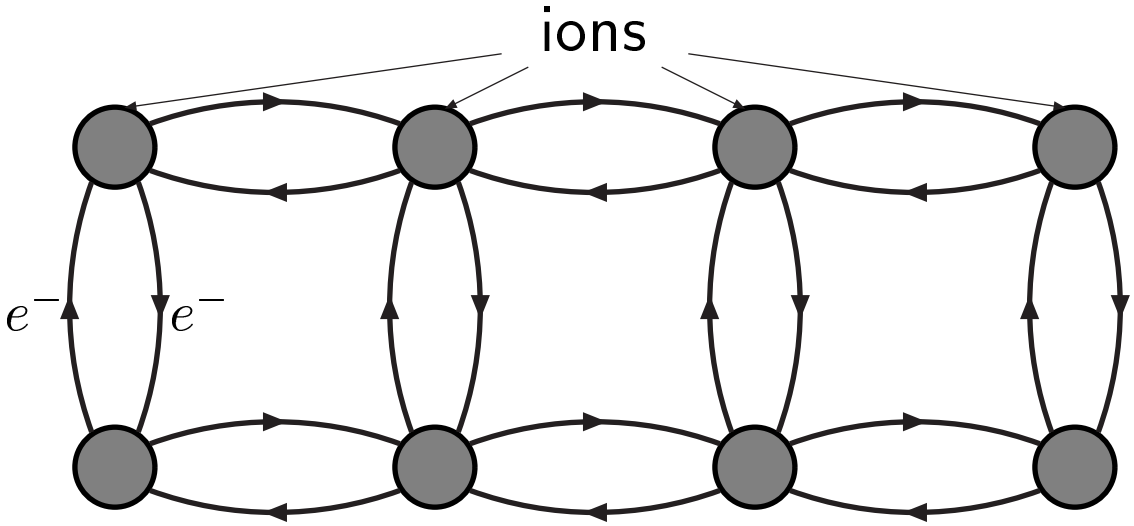

Two types of interaction:
1) Direct "perturbative" photon exchange.
2) "Non-perturbative" interaction through lattice (phonon exchange).

$$A^a_\mu = \frac{2}{g_s}\eta_{a\mu\nu}\frac{(x-x_0)_\nu}{(x-x_0)^2+\rho^2}$$

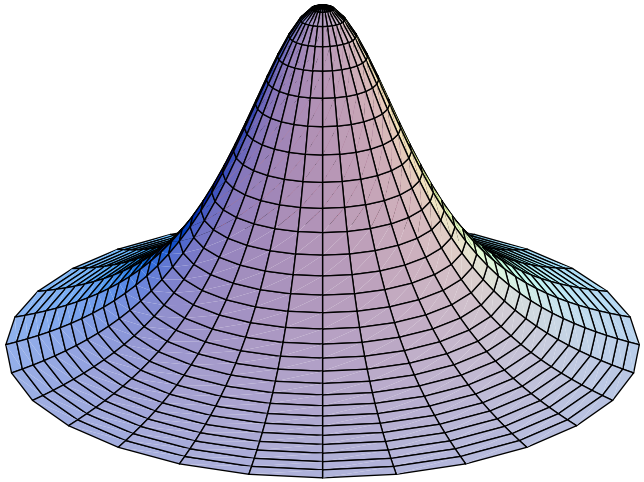

Figure 1: Instanton solution in QCD.

Quark-quark and quark-gluon interactions induced by instantons

Multiquark t'Hooft interaction induced by instantons

For N_f=3, $q = u, d, s \Rightarrow$ six-quark effective interaction induced by instantons

In $m_u = m_d = m_s \to 0$ limit

$$H_{t'Hooft} = \int d\rho n(\rho) \left(4\pi^2\rho^3\right)^3 \frac{1}{6N_C(N_C^2-1)} \varepsilon_{f_1 f_2 f_3} \varepsilon_{g_1 g_2 g_3} \times$$

$$\times \left\{ \frac{2N_C+1}{2N_C+4} \bar{q}_R^{f_1} q_L^{g_1} \bar{q}_R^{f_2} q_L^{g_2} \bar{q}_R^{f_3} q_L^{g_3} + \right.$$

$\frac{1}{N_C}$correction

$$\left. + \frac{3}{8(N_C+2)} \bar{q}_R^{f_1} q_L^{g_1} \bar{q}_R^{f_2} \sigma_{\mu\nu} q_L^{g_2} \bar{q}_R^{f_3} \sigma_{\mu\nu} q_L^{g_3} + (R \leftrightarrow L) \right\}$$

Very important in some processes: $K \to \pi\pi$ decays, $\Delta I = 1/2$ rule, CP violation, etc .. (N.K. and V.Vento, "Instantons and the Delta(I) = 1/2 rule," Phys. Rev. Lett. **87** (2001) 111601)

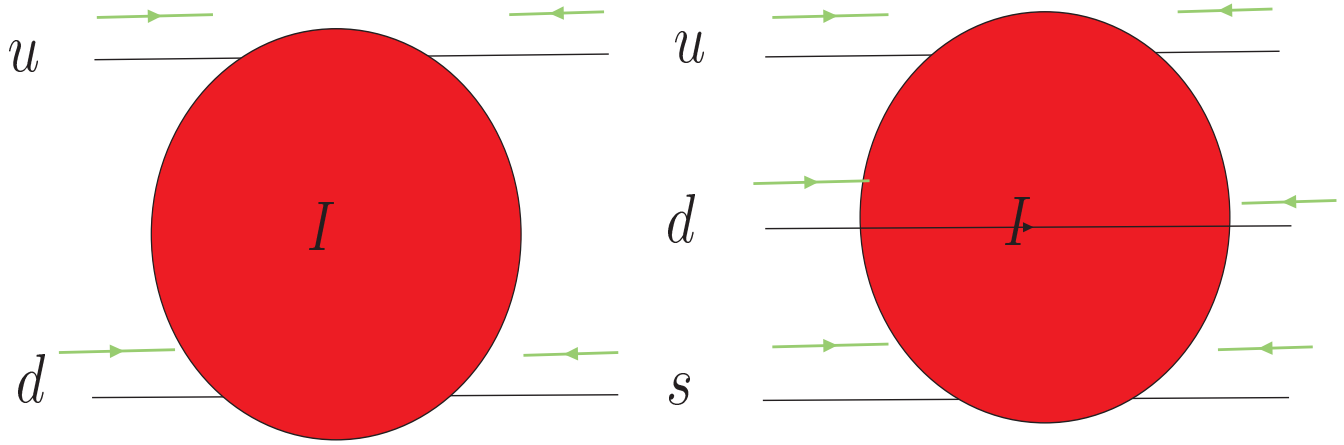

Figure 2: The quark-quark chirality-flip t'Hooft interaction induced instanton .

Quark-gluon interactions induced by instantons

• In the general case, the interaction vertex of massive quark with gluon can be written in the following form:

$$V_\mu(k_1^2, k_2^2, q^2)t^a = -g_s t^a[\gamma_\mu F_1(k_1^2, k_2^2, q^2) + \frac{\sigma_{\mu\nu}q_\nu}{2M_q}F_2(k_1^2, k_2^2, q^2)],$$

where $k_{1,2}^2$ are virtualities of incoming and outcoming quarks and q is momentum transfer.

It is similar to the photon-nucleon vertex

$$\Gamma_\mu{}^{QED} = \gamma_\mu F_1(q^2) + \frac{\sigma_{\mu\nu}q_\nu}{2M_N}F_2(q^2),$$

where $F_1(q^2), F_2(q^2)$ are Dirac and Pauli nucleon form factors, correspondently.

• Anomalous quark chromomagnetic moment (AQCM):

$$\mu_a = F_2(0, 0, 0).$$

$$\Delta\mathcal{L} = -\imath\mu_a \frac{g_s}{4M_q}\bar{q}\sigma_{\mu\nu}t^a q G^a_{\mu\nu}$$

$\mu_a \approx -0.4$ [N.K. 1996]
$\mu_a \approx -1.6$ [Diakonov 2002]

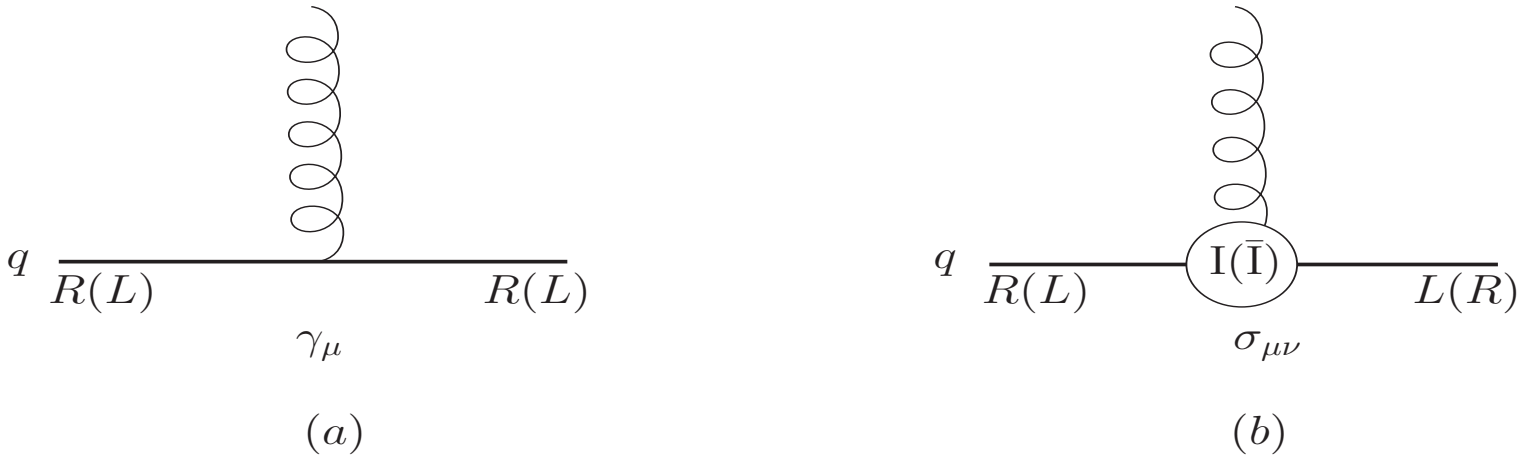

Figure 3: The quark-gluon coupling: a) perturbative and b) nonperturbative. Symbols R and L denote quark chirality and symbol $I(\bar{I})$ denotes instanton (antiinstanton).

The shape of form factor $F_2(k_1^2, k_2^2, q^2)$ within instanton model is fixed:

$$F_2(k_1^2, k_2^2, q^2) = \mu_a \Phi_q(\mid k_1 \mid \rho/2)\Phi_q(\mid k_2 \mid \rho/2) F_g(\mid q \mid \rho) \ ,$$

where

$$\begin{aligned} \Phi_q(z) &= -z\frac{d}{dz}(I_0(z)K_0(z) - I_1(z)K_1(z)), \\ F_g(z) &= \frac{4}{z^2} - 2K_2(z) \end{aligned}$$

are the Fourier-transformed quark zero-mode and instanton fields, respectively, and $I_\nu(z)$, $K_\nu(z)$,are the modified Bessel functions and ρ is the instanton size.
The value of AQCM is determined by the effective density of the instantons $n(\rho)$ in nonperturbative QCD vacuum (N.K. (1996))

$$\mu_a = -\pi^3 \int \frac{d\rho n(\rho)\rho^4}{\alpha_s(\rho)}.$$

Within Shuryak's instanton liquid model

$$n(\rho) = n_c \delta(\rho - \rho_c),$$

leads to AQCM which is proportional to the packing fraction of instantons $f = \pi^2 n_c \rho_c^4$ in vacuum

$$\mu_a = -\frac{\pi f}{\alpha_s(\rho_c)}.$$

By using the following relation between parameters of the instanton model

$$f = \frac{3}{4}(M_q \rho_c)^2,$$

we obtain

$$\mu_a = -\frac{3\pi (M_q \rho_c)^2}{4\alpha_s(\rho_c)}.$$

The dimensionless parameter $\delta = (M_q \rho_c)^2$ is one of the main parameters of the instanton model. It is proportional to the packing fraction of instantons in QCD vacuum $\delta \propto f \ll 1$, and is rather small. For a fixed value of average instanton size $\rho_c^{-1} = 0.6$ GeV it changes from $\delta^{MF} = 0.08$ for $M_q = 170 MeV$ in the mean field approximation to $\delta^{DP} = 0.33$ for $M_q = 345$ MeV within Diakonov-Petrov model. For the

strong coupling constant at the scale of instanton average size

$$\alpha_s(\rho_c) \approx 0.5,$$

we obtain the following values for AQCM:

$$\mu_a^{MF} \approx -0.4, \quad \mu_a^{DP} \approx -1.6$$

in the mean field approximation and in the DP approach, respectively.

AQCM is large !

Spin-spin quark interaction induced by anomalous quark chromomagnetic moment

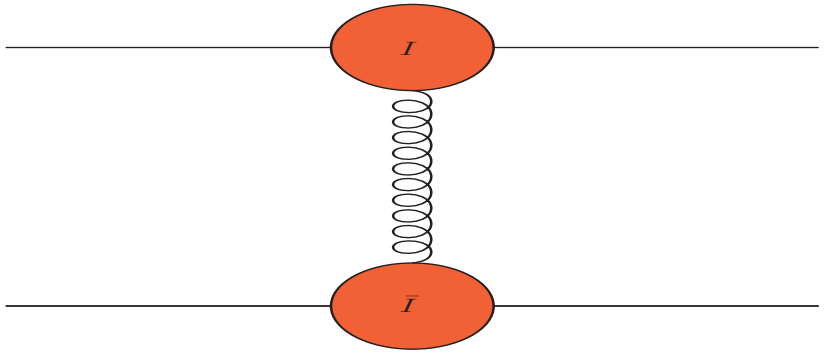

Figure 4: AQCM contribution to quark-quark scattering.

It is easy to show that AQCM existence leads to the spin-spin chromomagnetic interaction between light quarks which in the limit of small instanton size has the following form

$$V(\vec{r}) = -\frac{\pi\alpha_s\mu_1^a\mu_2^a}{6M_1M_2}\vec{\sigma_1}\vec{\sigma_2}\vec{\lambda_1}\vec{\lambda_2}\delta(\vec{r})$$

It is about factor three larger than pQCD one-gluon exchange contribution to Fermi-Breit interaction. Dominated contribution to the mass splitting between pion and ρ-meson, nucleon and Δ etc.

Soft Contribution to Quark-Quark Scattering coming from AQCM

N.K. JETP Lett. 83(2006)623

$$\frac{d\sigma^{chrom}}{dt} = \frac{2\mu_a^2|t|(F(\sqrt{|t|}\rho_c))^2}{M_q^2}\frac{d\sigma^{pert}}{dt}$$

where $F(\sqrt{|t|}\rho)$is instanton form factor

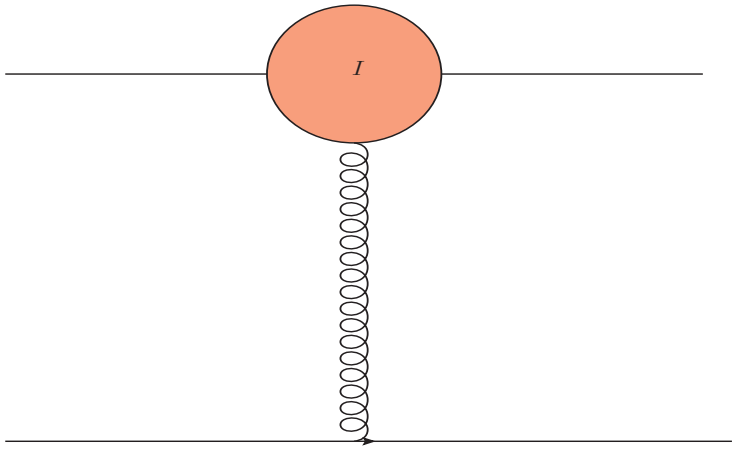

Figure 5: The Feynman diagram representing the contribution of the quark chromomagnetic moment to high energy spin-flip quark-quark scattering.

• The asymptotic behaviour of the nonperturbative contribution for large $p_\perp$ is determined by the instanton form factor

$$\frac{d\sigma^{chrom}}{dp_\perp} \approx \frac{const}{p_\perp^6},$$

• This $p_\perp$ dependence is steeper than is predicted by leading-twist pQCD, which anticipates $1/p_\perp^4$. The value $n^{chrom} = 6$ is in agreement with the result $n_{eff} = 6.33 \pm 0.54$ found in the recent analysis of RHIC data on inclusive neutral pion production. Violation of quark counting rule induced by complex structure of QCD vacuum.

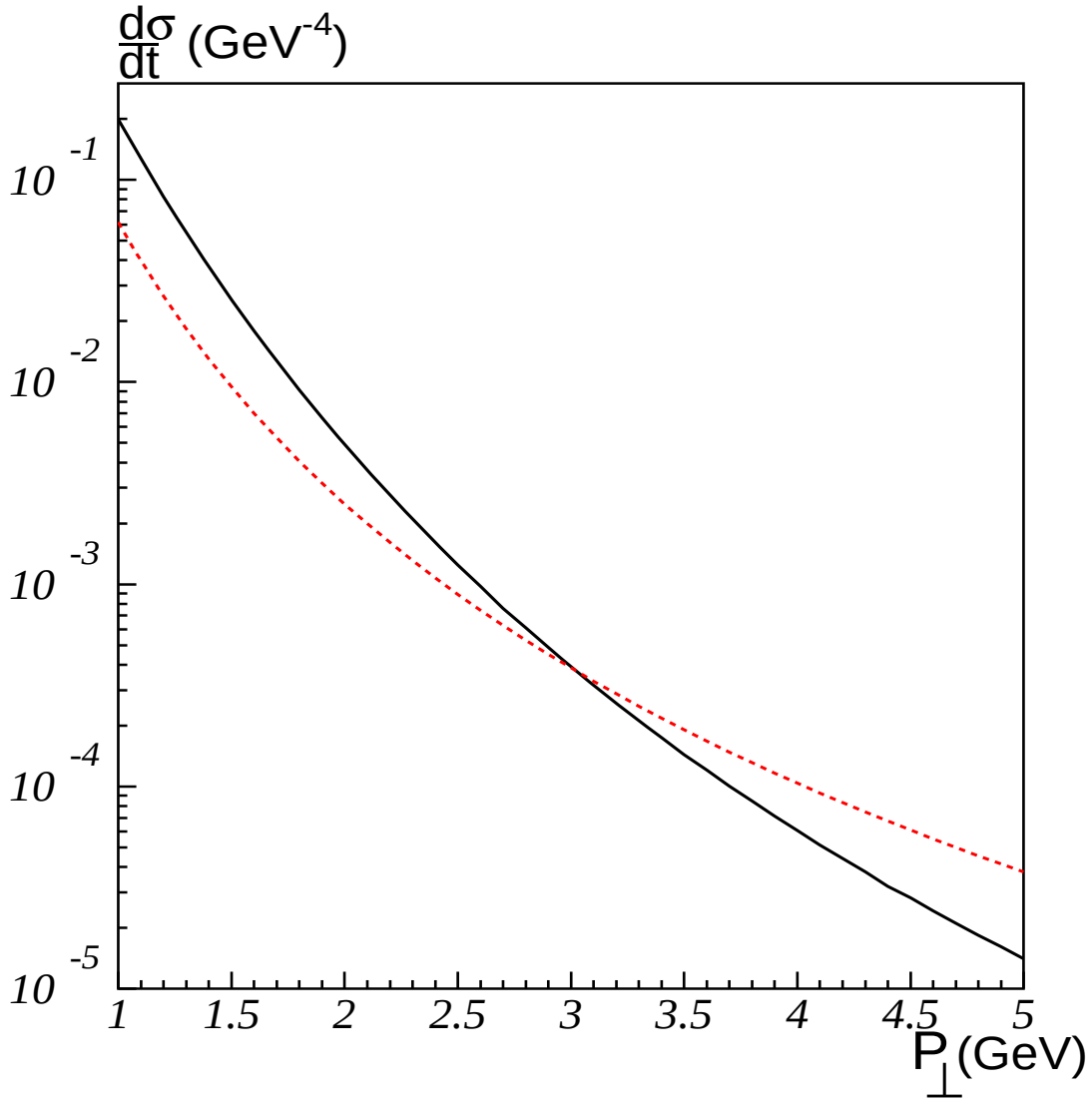

Figure 6: Perturbative (dashed) and nonperturbative (solid) quark-quark differential cross sections versus transverse momentum.

Pomeron structure

•Pomeron is effective colorless exchange between hadrons (quarks) which gives a dominated contribution to the high energy cross sections:

$$\sigma \approx s^{\alpha(0)_P - 1}$$

•Two types of Pomerons: "Soft" Landshoff and Nachtmann Pomeron for low virtuality of quark and gluons and intercept

$$\alpha_{soft}(0) \approx 1.08$$

and "Hard" Balitsky ,Kuraev, Lipatov and Fadin (BFKL) Pomeron: large virtualities and intercept

$$\alpha_{hard}(0) \approx 1.4.$$

Studies of pomeron properties at JINR: Selugin, Goloskokov, Kuraev, Kotikov, Uzhinskii

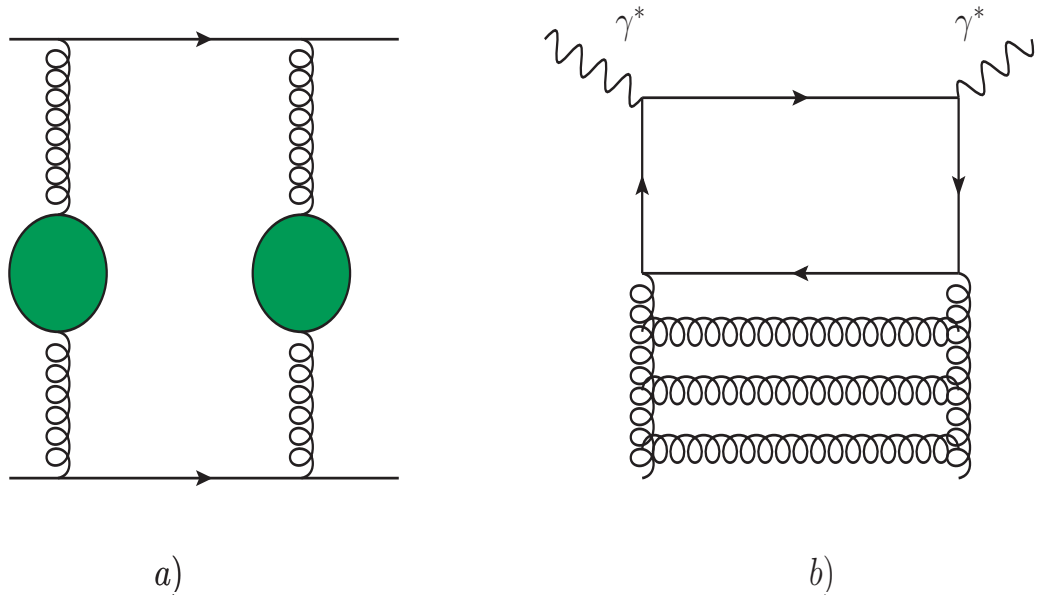

Figure 7: a) Soft Pomeron with non-perturbative gluon propagator in hadron-hadron scattering and b) Hard perturbative Pomeron in DIS.

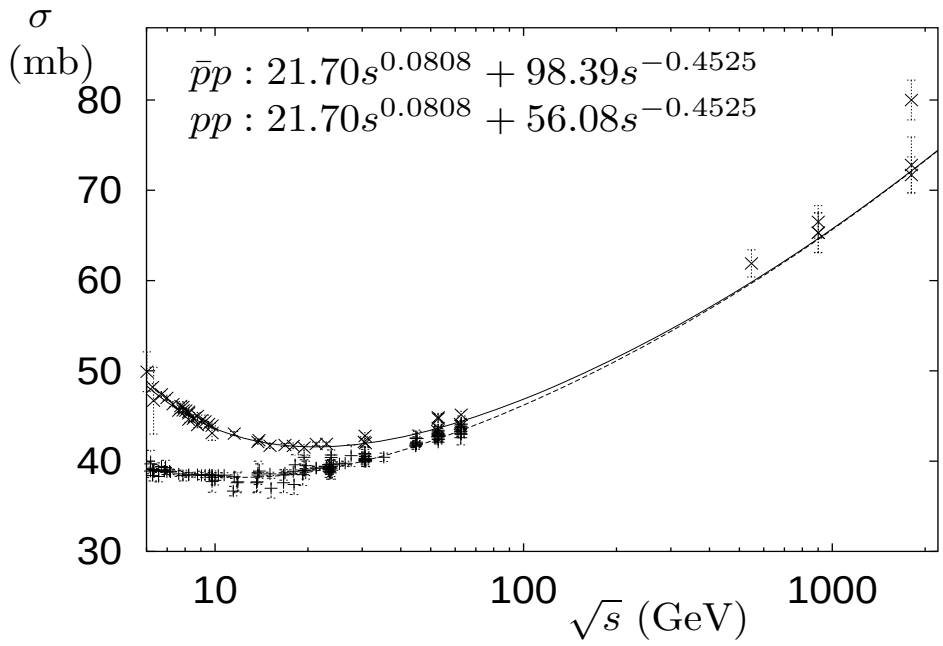

Figure 8: Soft Pomeron in pp and $\bar{p}p$ total cross sections.

Form factor in the first term in general quark-gluon vertex might be chosen in the form

$$F_1(k_1^2, k_2^2, q^2) = \Theta(\mid k_1^2 \mid + \mid k_2^2 \mid + \mid q^2 \mid -3\mu^2),$$

where μ is the factorization scale between perturbative and nonperturbative regimes. In our estimation below we will use $\mu \approx 1/\rho_c \approx 0.6$ GeV.

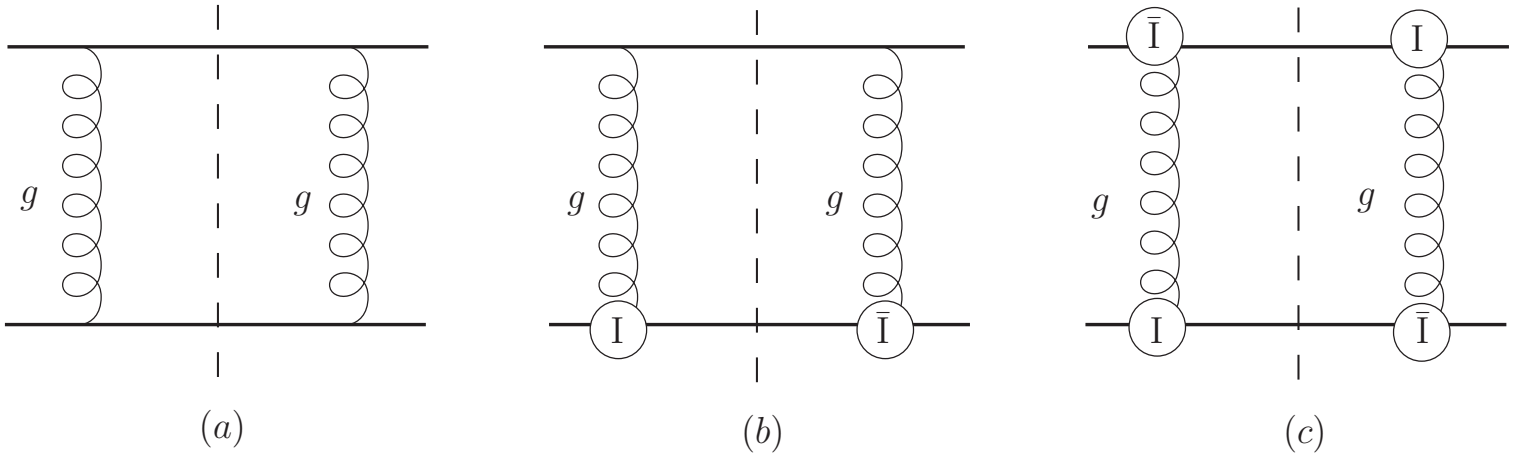

Figure 9: The fine pomeron structure in the model with perturbative and nonperturbative interactions: a) perturbative contribution, b) interference perturbative and nonperturbative vertices, c) nonperturbative contribution. The symbol I ($\bar{I}$) denotes instanton (antiinstanton).

The total contribution to quark-quark cross section for the quarks with small virtualities is

$$\sigma^{total} = \sigma^{pert} + \sigma^{mix} + \sigma^{nonpert}, \tag{1}$$

where

$$\sigma^{i} = \int_{q^2_{min}}^{q^2_{max}} \frac{d\sigma^{i}(t)}{dt} dq^2, \tag{2}$$

$$\begin{aligned}
\frac{d\sigma(t)^{pert}}{dt} &= \frac{8\pi\alpha_s^2(q^2)}{9q^4} \\
\frac{d\sigma(t)^{mix}}{dt} &= \frac{\alpha_s(q^2)\pi^2 \mid \mu_a \mid \rho_c^2 F_g^2(|q|\rho_c)}{3q^2} \\
\frac{d\sigma(t)^{nonpert}}{dt} &= \frac{\pi^3 \mu_a^2 \rho_c^4 F_g^4(|q|\rho_c)}{32},
\end{aligned}$$

where $q^2 = -t$ and $q^2_{min} \approx 1/\rho_c^2$ for pQCD and mixed contributions. For pure nonperturbative contribution $q^2_{min} = 0$.

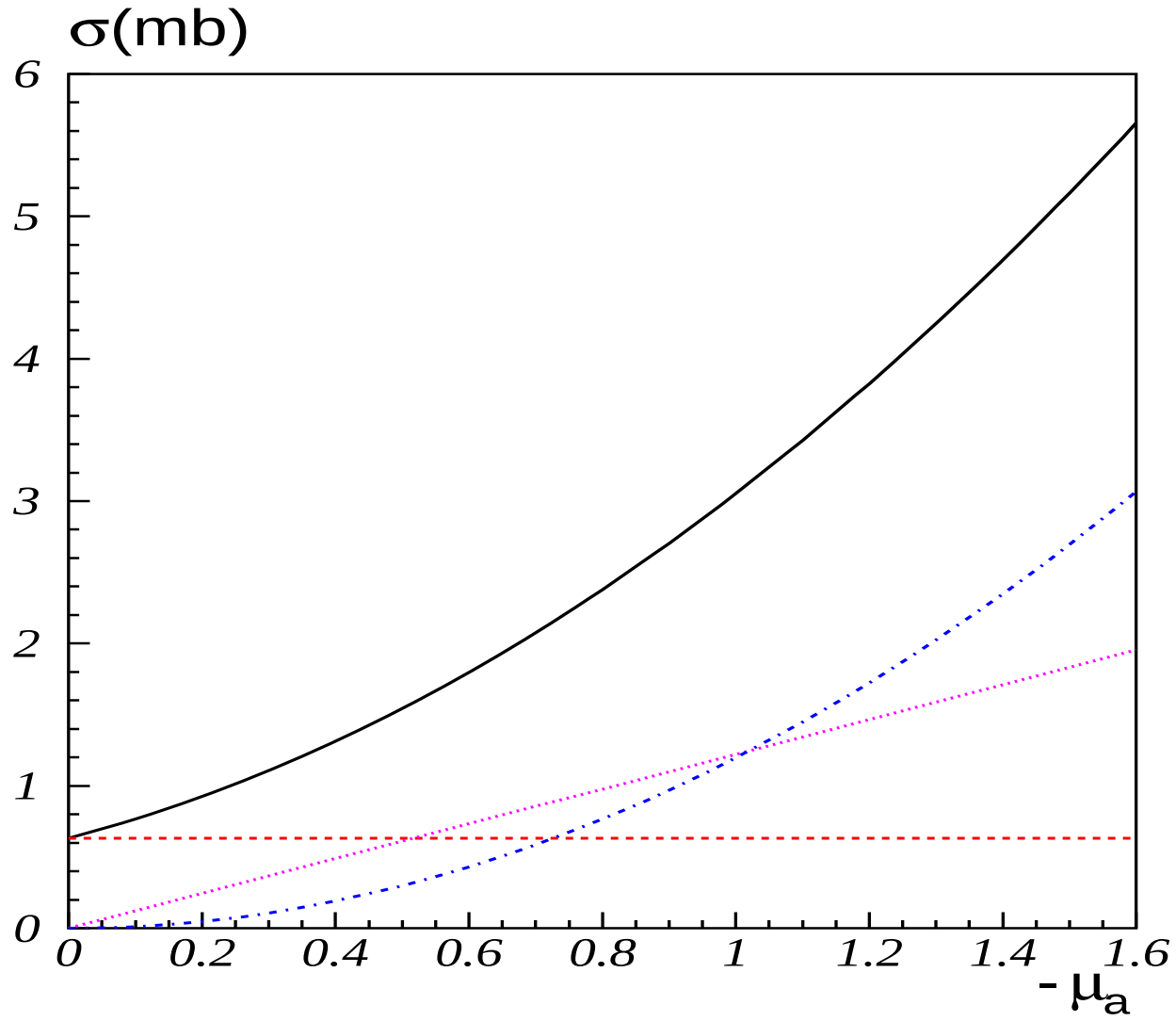

Figure 10: The contibution to the total quark-quark cross section as a function of AQCM: perturbative (dashed line) , mixed (dotted line), nonperturbative (dashed-dotted line) and their sum (solid line).

For the strong coupling constant, the following parametrization was:

$$\alpha_s(q^2) = \frac{4\pi}{9\ln((q^2+m_g^2)/\Lambda^2_{QCD})},$$

where $\Lambda_{QCD} = 280$ MeV and the value $m_g = 0.88$ GeV was fixed from the requirement $S_0 = 2\pi/\alpha_s(q^2 = 1/\rho_c^2) \approx 12$ as in Shuryak-Diakonov-Petrov instanton liquid model. This form for $\alpha_s(q^2)$ describes the frozen coupling constant in the infrared region, $\alpha_s(q^2) \to constant$ as $q^2 \to 0$.

From hadron spectroscopy (Faustov, Galkin, Ebert) obtained $\mu_a \approx -1$. In our calculation it corresponds to the value of dynamical quark mass $M_q = 280$ MeV. For such μ_a we have got $\sigma_{qq}^{tot} = 3.05$ mb.
That number is not far away from $\sigma_{qq}^{exp} = 4$ mb (inelastic $\sigma_{pp(\bar{p})}^{exp} \approx 36$ mb in the energy range where $pp(p\bar{p})$ cross sections are approximately constant).

- Two types of Pomerons:

- a) "Soft" Pomeron (quark virtuality is small):Intermediate spin-flip chromomagnetic interaction induced by vacuum gluonic instanton field. For heavy quarks there is suppression $1/{m_q}^2$.

- b) "Hard" Pomeron (quark virtuality is large): No spin-flip in intermediate state. There is no suppression for heavy quarks.

Dynamics of elastic PP and $P\bar{P}$ scattering

Included into current and future accelerator programs: NICA (Russia), J-Park (Japan), PAX (FAIR,Germany), TOTEM (LHC, CERN).

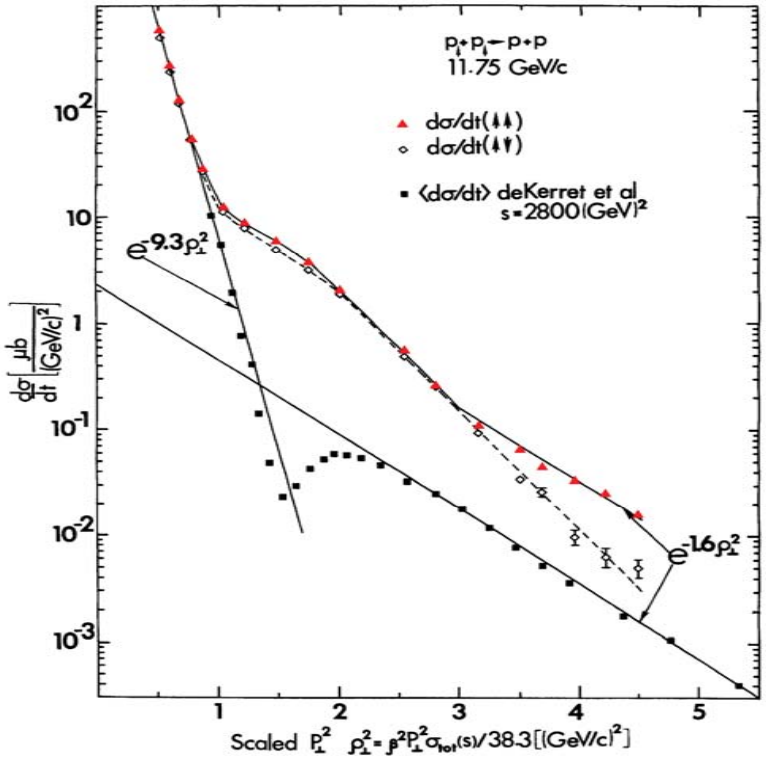

Figure 11: Differential cross-section of PP elastic scattering and its spin dependence (from A.D.Krisch, arXiv:1001.0790).

Odderon properties

Within the conventional approach, the Odderon P=C=-1 partner of Pomeron, originates from three gluon exchange with non-spin-flip perturbative-like quark-gluon vertex. The experimental support of the existence of such exchange comes from high energy ISR data on the difference in the dip structure around $\mid t \mid \approx 1.4$ GeV between the proton-proton and proton-antiproton differential cross section. However, there is no any signal for the Odderon at very small transfer momentum t.

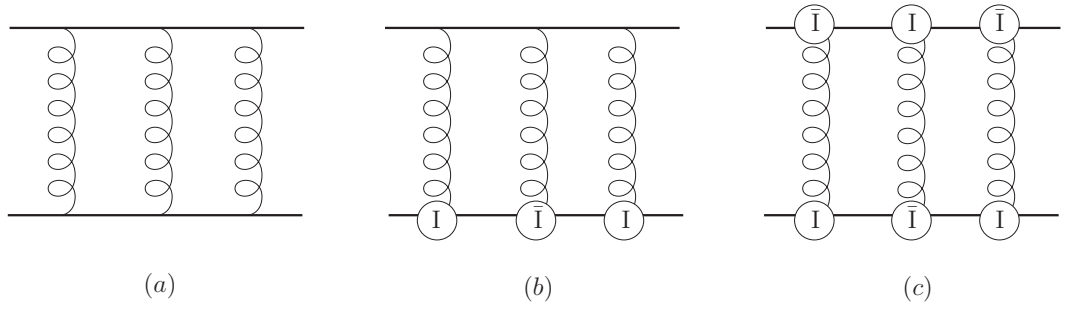

centerline

Figure 12: The structure of Odderon exchange: a) non spin-flip perturbative three gluon exchange, b) and c) nonperturbative spin-flip contributions.

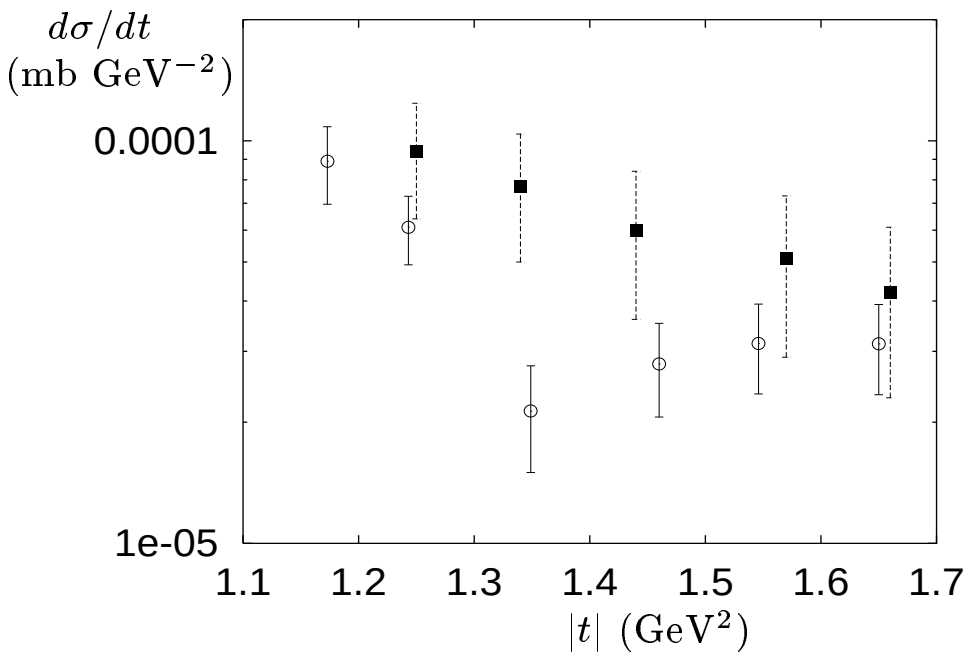

Figure 13: pp(lower points) and $\bar{p}p$(upper points) differential cross sections at $\sqrt{s} = 53$ GeV.

Quark-counting rule and Landshoff mechanism for elastic hadron-hadron scattering at large momentum transfer

• **Quark-counting rule (Matveev, Muradyan, Tavkelidze and Brodsky, Farrar (1973)) Differential cross-section for the scattering $AB \to CD$ at large S and $-t$ and $S \sim -t$ depends on the total number of valence quark in hadrons**

$$\frac{d\sigma}{dt} \sim s^{-n} f(\Theta)$$

where $n = n_A + n_B + n_c + n_D - 2$ and Θ is c.m. scattering angle. It comes from consideration of pQCD *connected* graphs.
For $PP \to PP$ $n = 10$ (fixed target experiment at AGS at low energy $p = 5.9$ GeV/c gives $n = 9.1 \pm 0.2$)

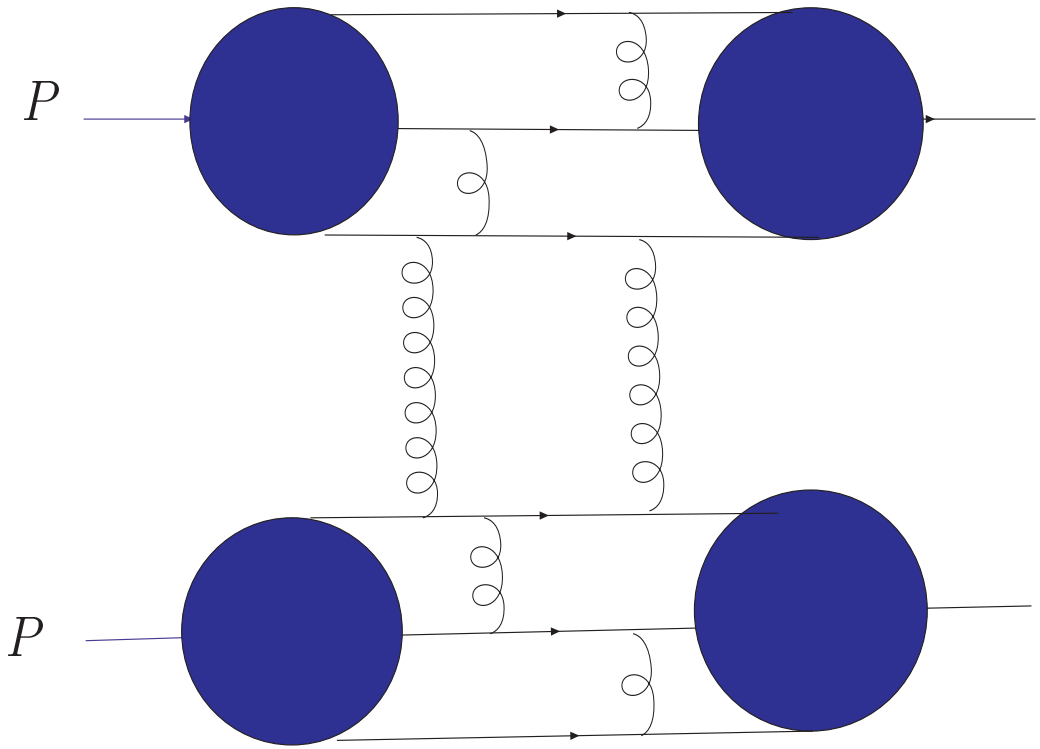

Figure 14: The example of pQCD contribution coming from the connected diagrams to the PP elastic scattering which leads to the quark-counting rule.

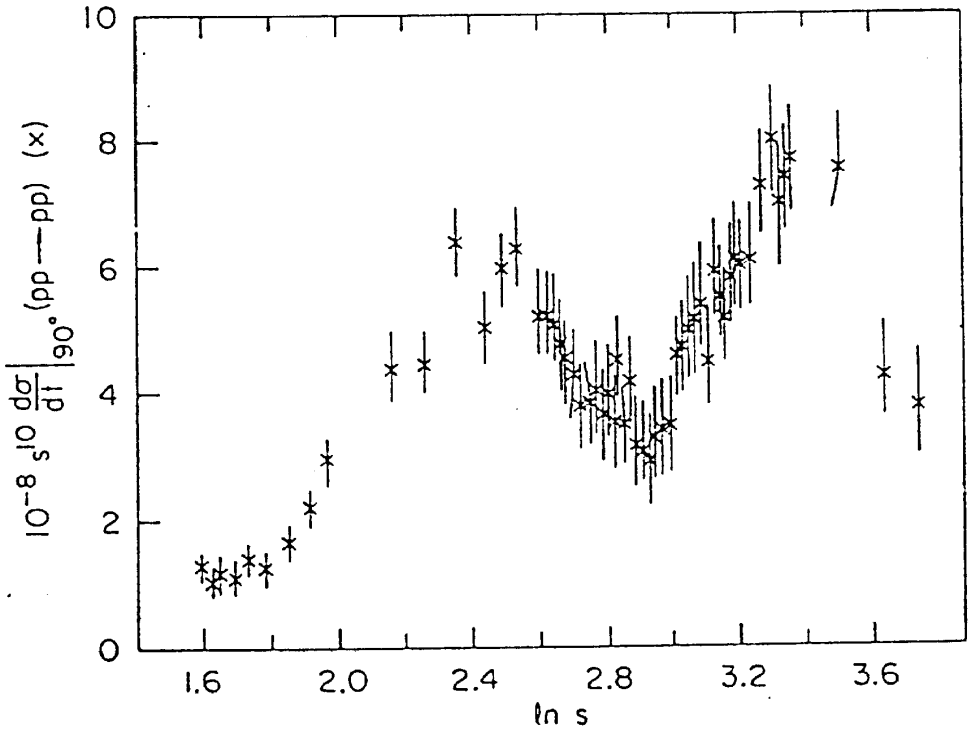

Figure 15: Deviation from quark-counting rule for differential cross-section of elastic PP scattering at 90° as the function of the energy (from Sivers et. al. Phys.Rep. **23** (1976) 1).

Landshoff's perturbative and nonperturbative mechanism for elastic hadron-hadron scattering at large momentum transfer

At large $S \gg -t$ and large $-t \gg M_P^2$ the differential cross section of PP and $P\bar{P}$ $d\sigma/dt$ does not depend on the energy.

Landshoff mechanism for large $q^2 = -t$ hadron-hadron scattering-contribution from disconnected diagrams (each gluon carries about $q/3$ transfer momentum).

Donnachie, Landshoff Z.Phys. C2 (1979)55 (D-L model)

According to our model, the perturbative part of the Odderon in the region of momentum transfer $on\ quark\ level!$ $p_\perp^{qq} \leq 3$ GeV ($-t^{qq} \leq 9$ GeV^2) is expected to be much smaller in comparison with the nonperturbative AQCM part. Elastic $PP \to PP$ at large $-t \geq 3$ GeV^2 in D-L model.

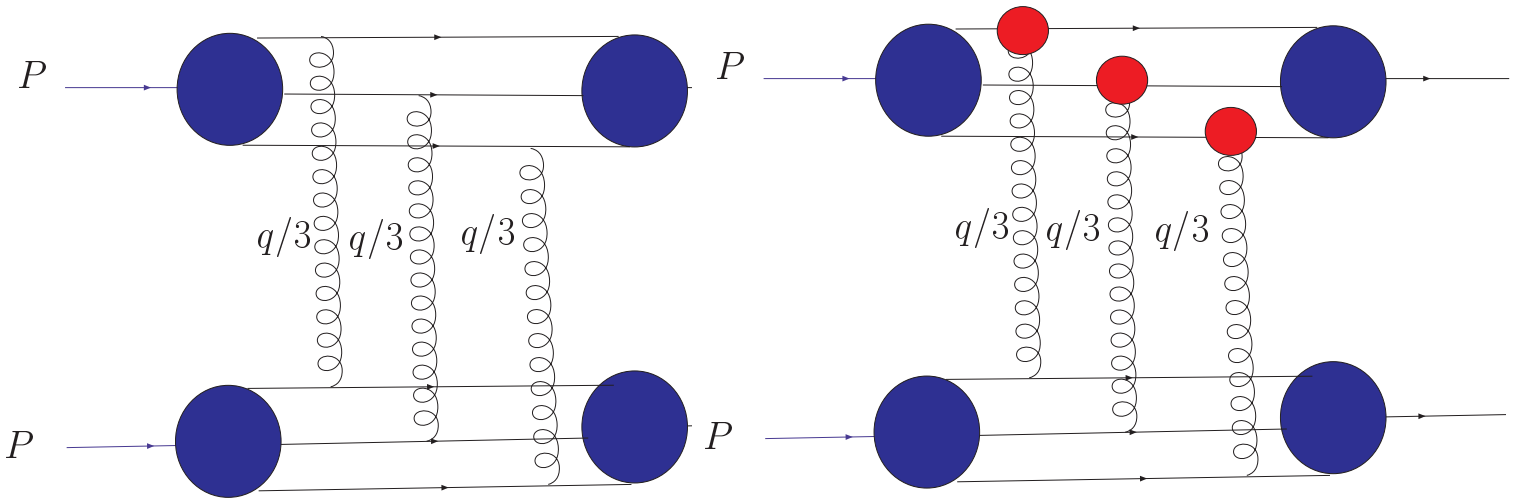

Figure 16: The left panel is Landshoff mechanism for large $-t$ nucleon-nucleon scattering. The right panel is an example of AQCM contribution.

$$\frac{d\sigma}{dt} \sim \frac{244P^4}{S^6t^2R^{12}} \mid M_{qq}(\Theta) \mid^6 \sim \frac{1}{t^2(t^2)^3} \sim \frac{1}{t^8},$$

where $S = (p_1 + p_2)^2$ and t is transfer momentum, P^2 is probability of

three quark configuration in proton and R is proton radius.

$$\mid M_{qq}^{pQCD}(\Theta) \mid^2 = \frac{128\pi^2\alpha_s^2}{9}\frac{\hat{s}^2}{\hat{t}^2},$$

where on the quark level $\hat{s} \approx S/9$, $\hat{t} \approx t/9$
and at $\hat{s} >> -\hat{t}$ $\hat{s}/\hat{t} \sim -4/sin^2(\Theta)$. In D-L estimation they use $ad\ hoc$:
$P = 1/10$, $\alpha_s = 0.3$ and $R^{-1} = 640$ MeV.
Very small proton radius $R \approx 0.3fm$!
If we take $P = 1$ and $R = 1$ fm we have got for $\alpha_s = 0.3$ $d\sigma/dt \sim 8 \cdot 10^{-4}/t^8$ mb/GeV^2 (two orders of magnitude less than the experiment: $\approx 9 \cdot 10^{-2}/t^8$ mb/GeV^2.)
AQCM contribution:

$$\begin{aligned}\mid M_{qq}^{AQCM}(S,t) \mid^2 &= \frac{4\pi^4 \mid \mu_a \mid \alpha_s(\mid \hat{t} \mid)}{9\alpha_s(\rho_c)}\frac{S^2}{\mid t \mid}(M_q\rho_c)^2\rho_c^2F_g^2(\sqrt{\mid t \mid}\rho_c/3) \\ &\quad +9\pi^4\mu_a^2\rho_c^4S^2F_g^4(\sqrt{\mid t \mid}\rho_c/3),\end{aligned}$$

Inspite of the fact that AQCM contribution asymptotically decays as $1/t^{11}$ it describes the existent large $-t$ data very well.

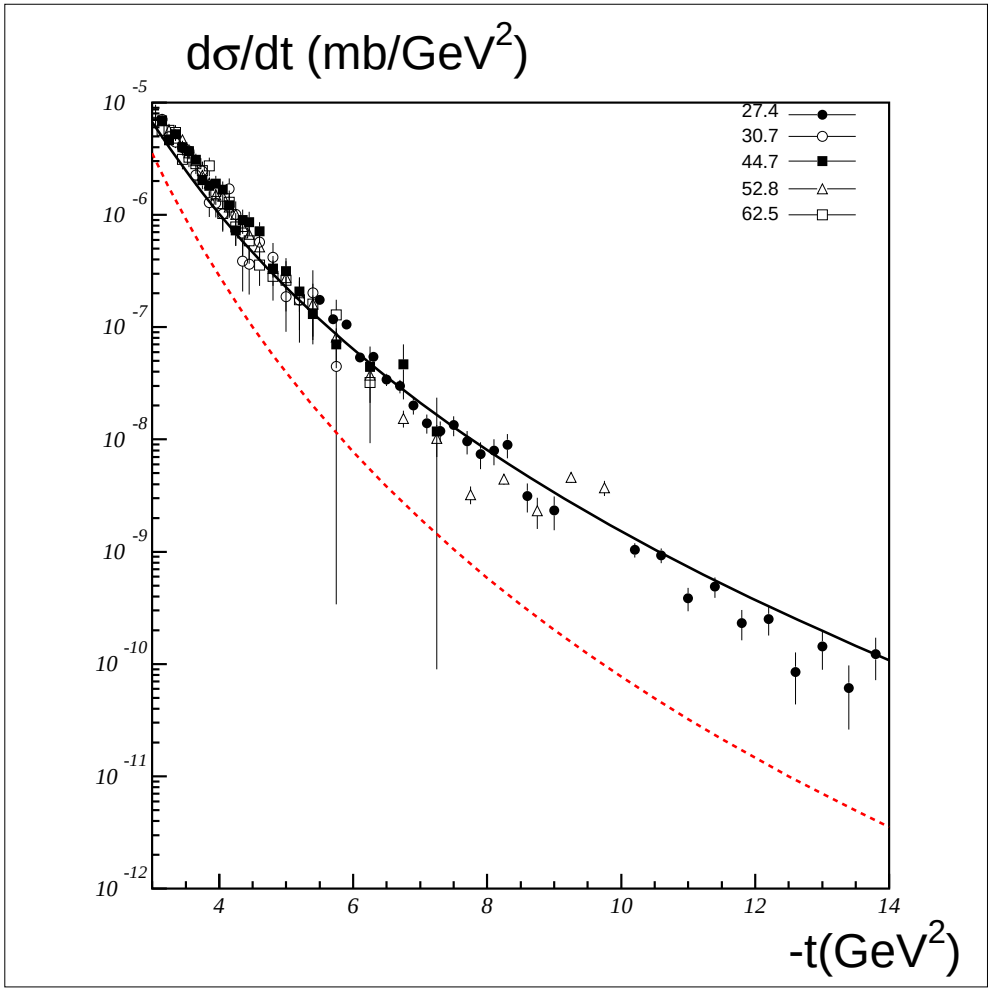

Figure 17: The contribution of pQCD exchange (dashed line) and AQCM contribution (solid line) to elastic proton-proton scattering at large energy and large momentum transfer.

Single-spin asymmetry A_N in PP and $P\bar{P}$ elastic scattering

$$A_N = -\frac{2Im[\Phi_5^*(\Phi_1+\Phi_2+\Phi_3-\Phi_4)]}{\mid\Phi_1\mid^2+\mid\Phi_2\mid^2+\mid\Phi_3\mid^2+\mid\Phi_4\mid^2+4\mid\Phi_5\mid^2},$$

where helicity amplitudes $\Phi_1 =< ++ \mid ++ >$, $\Phi_2 =< ++ \mid -- >$, $\Phi_3 =< +- \mid +- >$, $\Phi_4 =< ++ \mid -- >$ and $\Phi_5 =< ++ \mid -+ >$.

- **Spin-flip dominance in Odderon amplitude: $\Phi_5 =< ++ \mid -+ >$ amplitude is very large.**

- **Due to spin-flip the contribution of Odderon to the difference of PP and $P\bar{P}$ differential cross sections at $-t = 0$ is zero at high energies!**

- **Interference with spin-flip part of Pomeron amplitude at large $-t$. Difference in PP and $P\bar{P}$ cross sections in dip region $-t \sim 1-2$ GeV**

- **Large asymmetry A_N in PP and $P\bar{P}$ elastic scattering with**

opposite sign between them! The opposite sign for A_N in elastic $P\bar{P}$ can be checked at FAX Collaboration at FAIR.

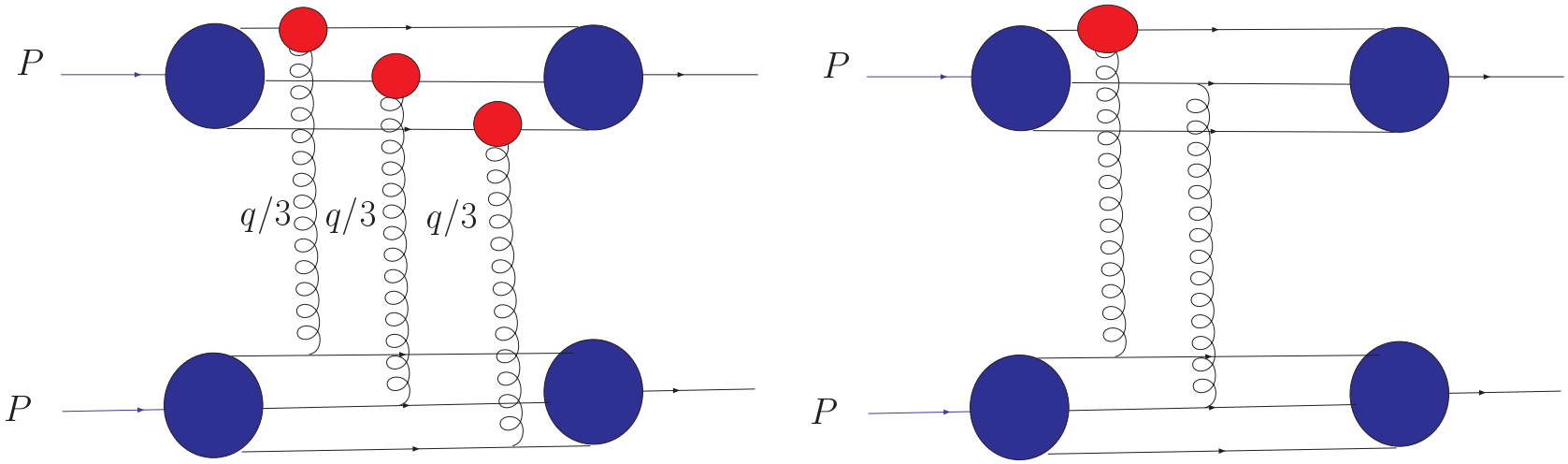

Figure 18: The interference between Landshoff-type AQCM diagram and pomeron spin-flip induced by AQCM.

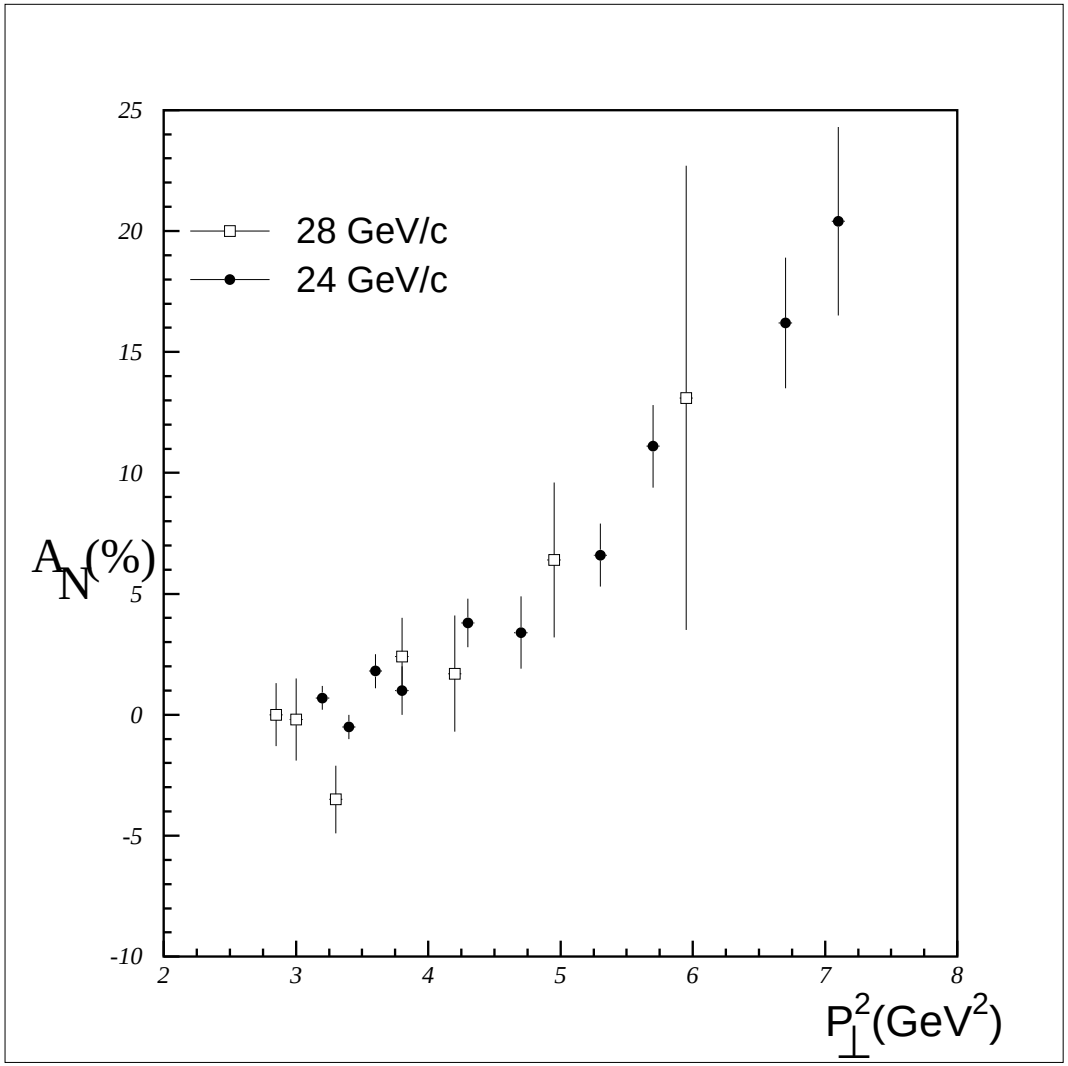

Figure 19: Single-spin asymmetry in the elastic $PP \to PP$ scattering at large momentum transfer at AGS.

Non-factorizable contribution to inclusive meson production

$1/N_c$ correction to AQCM quark-gluon interaction-PCAC requirement. Non-linear σ model (pion part) from t'Hooft interaction (Diakonov,Petrov etc.):

$$\mathcal{L}_{eff} = \bar{q}[i\hat{\partial} - M_q e^{i\gamma_5 \vec{\tau}\vec{\pi}/F_\pi}]q$$

Expansion to AQCM contribution (Diakonov 2003):

$$\Delta\mathcal{L}_{eff} = -\imath\mu_a \frac{g_s}{4M_q}\bar{q}\sigma_{\mu\nu}e^{i\gamma_5\vec{\tau}\vec{\pi}/F_\pi}t^a q$$

Direct meson production by instanton field-NO FRAGMENTATION FUNCTION!
(Kochelev and Korchagin to be published)

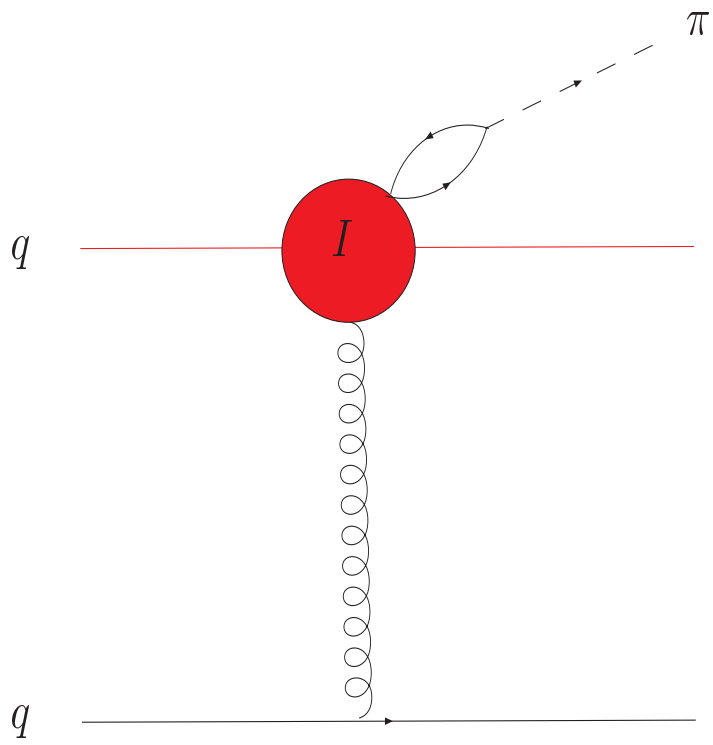

Figure 20: "Direct" π-meson production in instanton field.

Single-spin asymmetries in high energy reactions

In perturbative QCD single-spin asymmetries are expected to be very small

$$A_N \approx \frac{\alpha_s m_{curr}}{p_\perp}$$

Large single-spin asymmetries were observed in many hadron reactions

Different mechanisms, mainly based on the factorization, have been suggested: twist-3 (Efremov, Teryaev), Sivers distribution and Collins fragmentation functions etc.

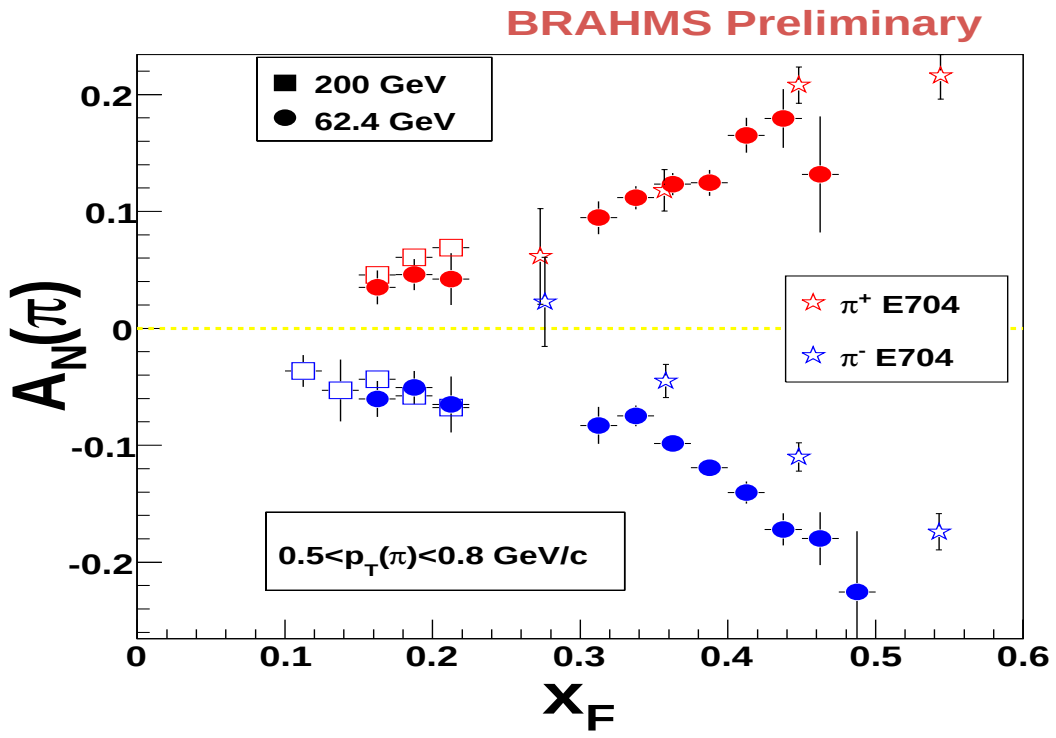

Figure 21: Comparison of charged pion asymmetries measured at 200 and 62.4 GeV by the BRAHMS experiment and at 19.4 GeV by the E704 experiment.

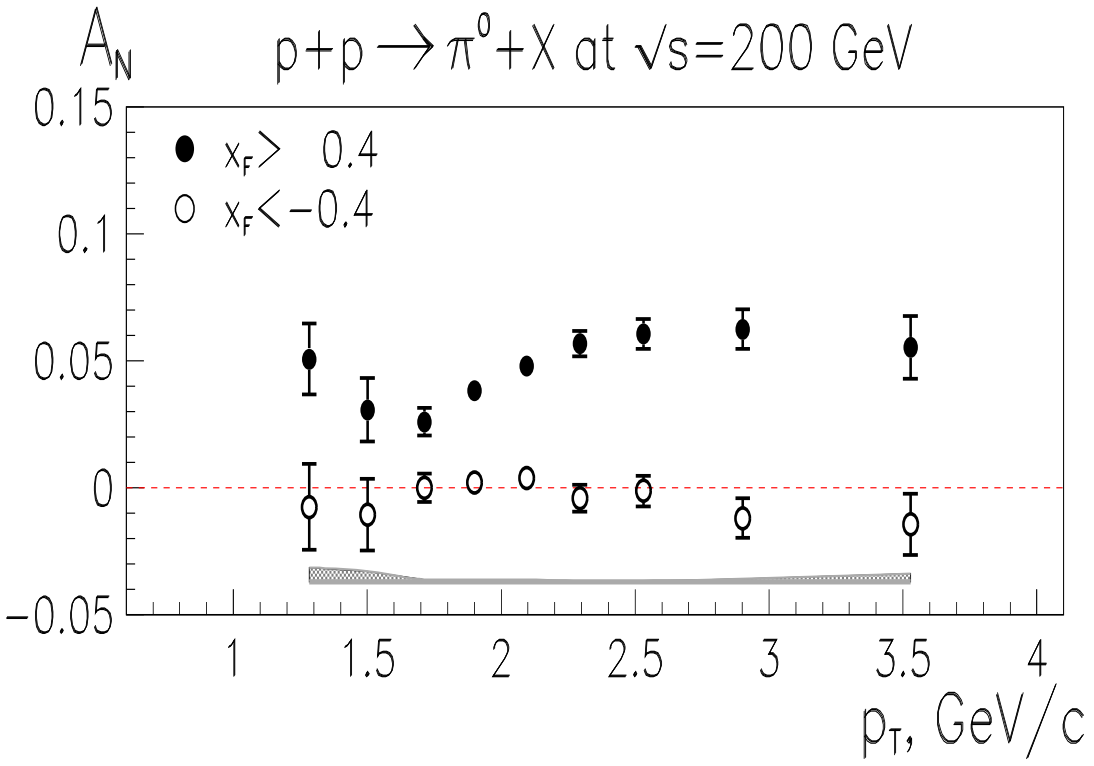

Figure 22: STAR experiment SSA data at $\sqrt{s} = 200$ GeV for neutral pions as the function of $P_{h\perp}$.

STAR new data for η SSA

•Reaction

$$p\uparrow + p \to M + X, \quad M \to \gamma\gamma$$

at very large energy $\sqrt{S} = 200$ GeV.

• Very large asymmetry for η meson !!!
$< A_N >_\eta = 0.361 \pm 0.064$
(flavor content $\eta = \frac{1}{\sqrt{6}}(u\bar{u} + d\bar{d} - 2s\bar{s})$)
in comparison with π^0 SSA
$< A_N >_{\pi^0} = 0.078 \pm 0.018$ in the interval $0.55 < x_F < 0.75$.
(flavor content $\pi^0 = \frac{1}{\sqrt{2}}(u\bar{u} - d\bar{d})$)

• Large negative SSA for neutron production (about 10%) at large $x_F \to 1$ and small $p_T < 100$ MeV was observed by PHENIX Collaboration at RHIC at $\sqrt{S} = 200GeV$

AQCM and single-spin asymmetries

• Two important ingredients should be in the game to explain a large single-spin asymmetries: large spin-flip amplitude and large imaginary part of non-spin-flip amplitude.

• Both of them have a natural origin coming from large AQCM. The sign of single-spin asymmetry is fixed by the sign of AQCM !

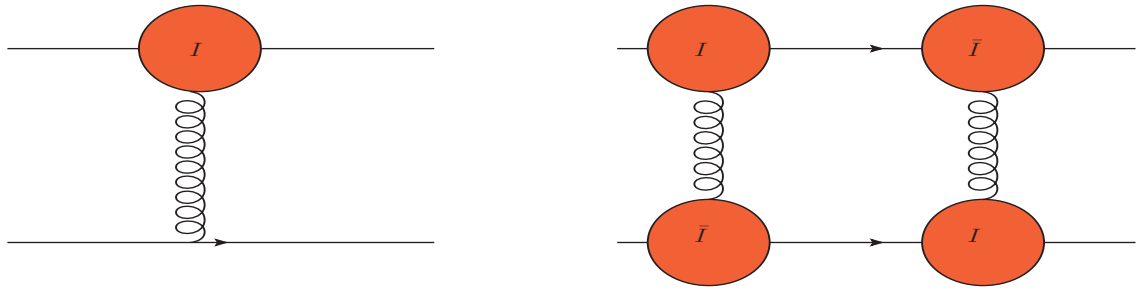

Figure 23: AQCM factorizable contribution to low $p_\perp$ high twist single-spin asymmetry in quark-quark scattering.

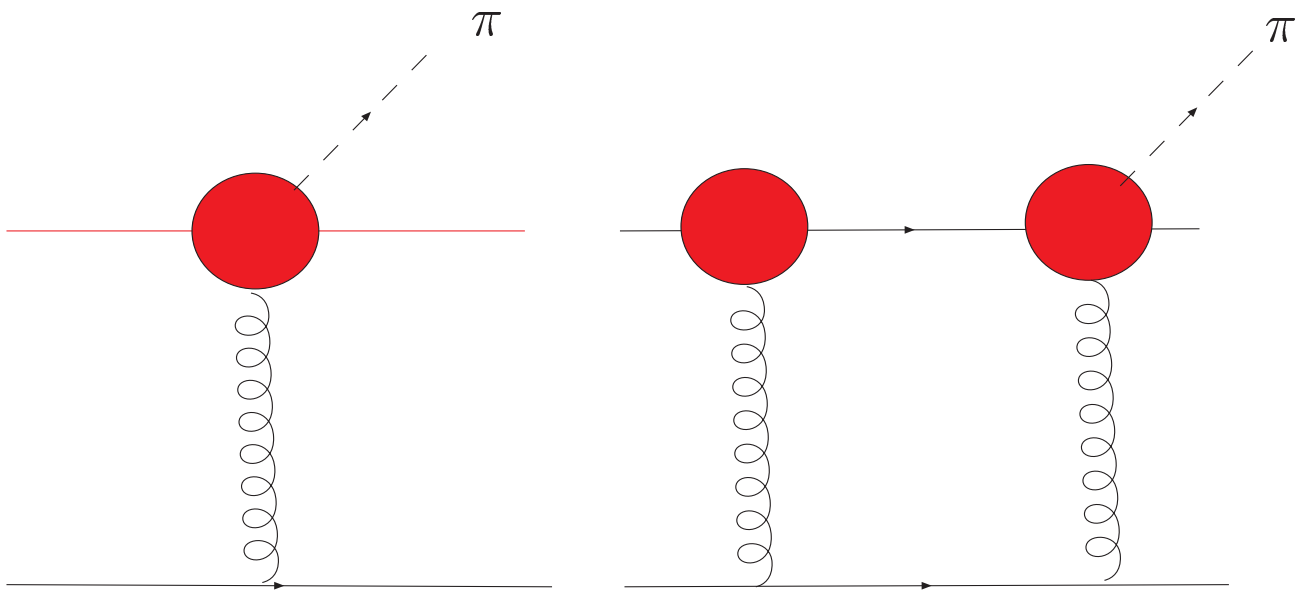

Figure 24: AQCM nonfactorizable contribution to large $p_\perp$ single-spin asymmetry for inclusive pion production in quark-quark scattering.

Nonperturbative energy loss by fast parton in strongly interacted Quark-Gluon Plasma

• Strongly interacted Quark-Gluon Plasma (sQGP) produced at high energy heavy ion collision.

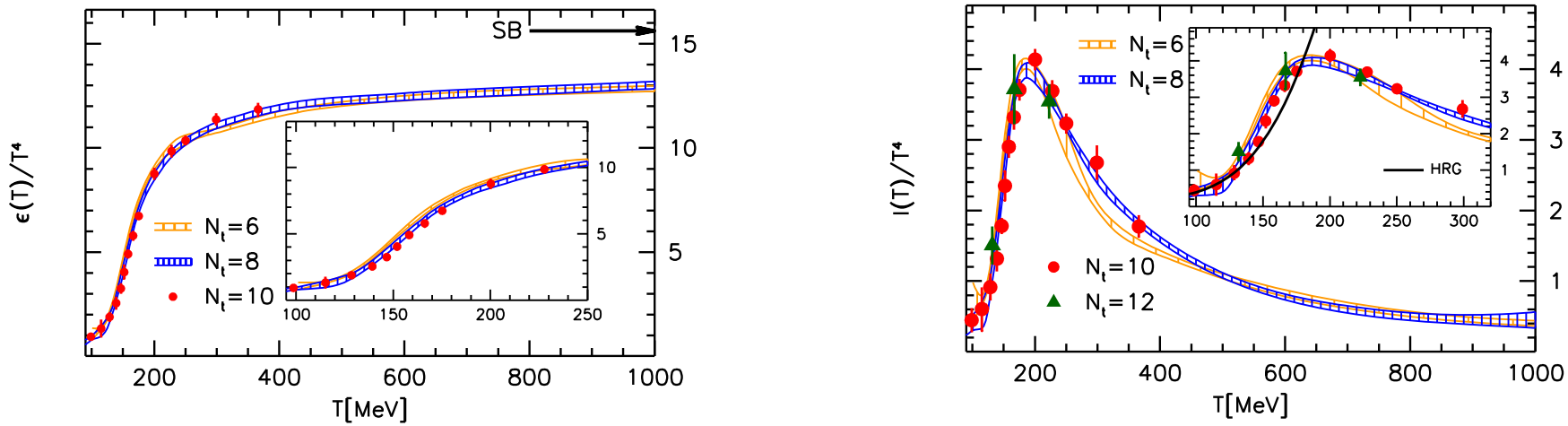

Figure 25: Right: Lattice calculation with dynamical quarks of scale anomaly $I = \epsilon - 3p$. Left: Energy density as the function of temperature. Results are taken from the paper by S.Borsanyi et al. JHEP **1011** (2010) 077 (Germany-Hungary-USA Collaboration).

• Secondary particle production suppression factor and jet quenching as a tool for investigation of the Quark-Gluon Matter created in high energy heavy ion collision.

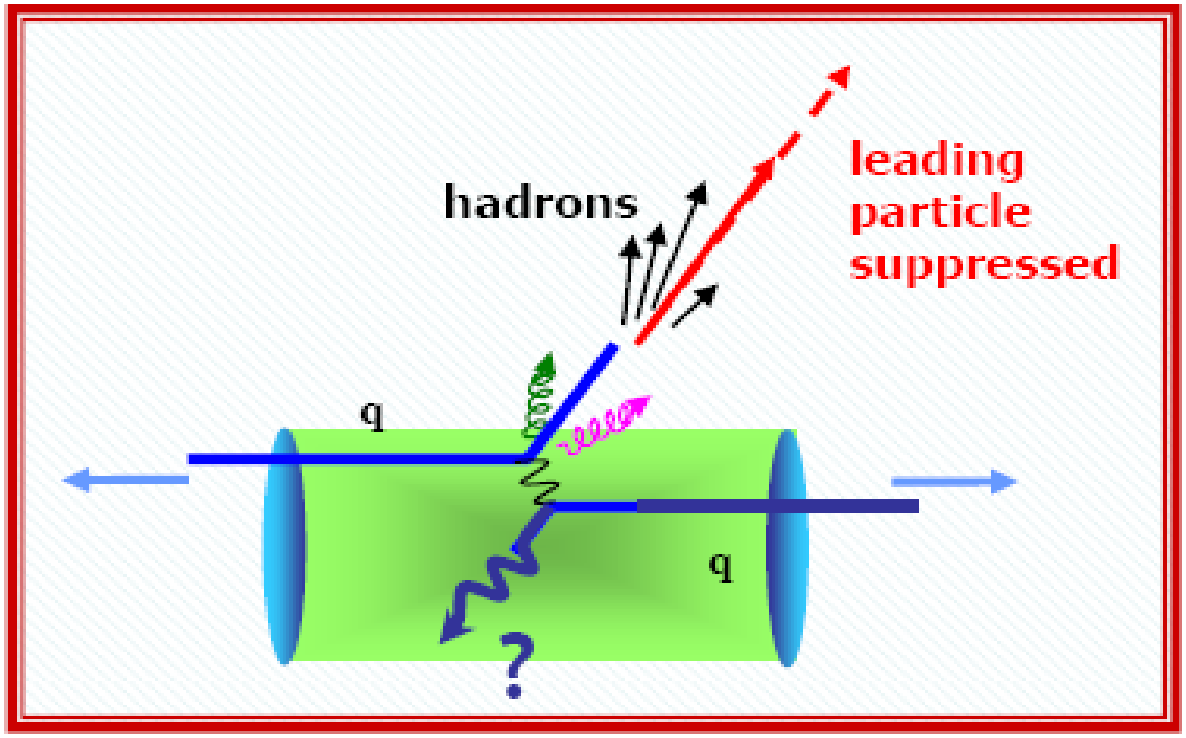

Figure 26: Nuclear modification factor

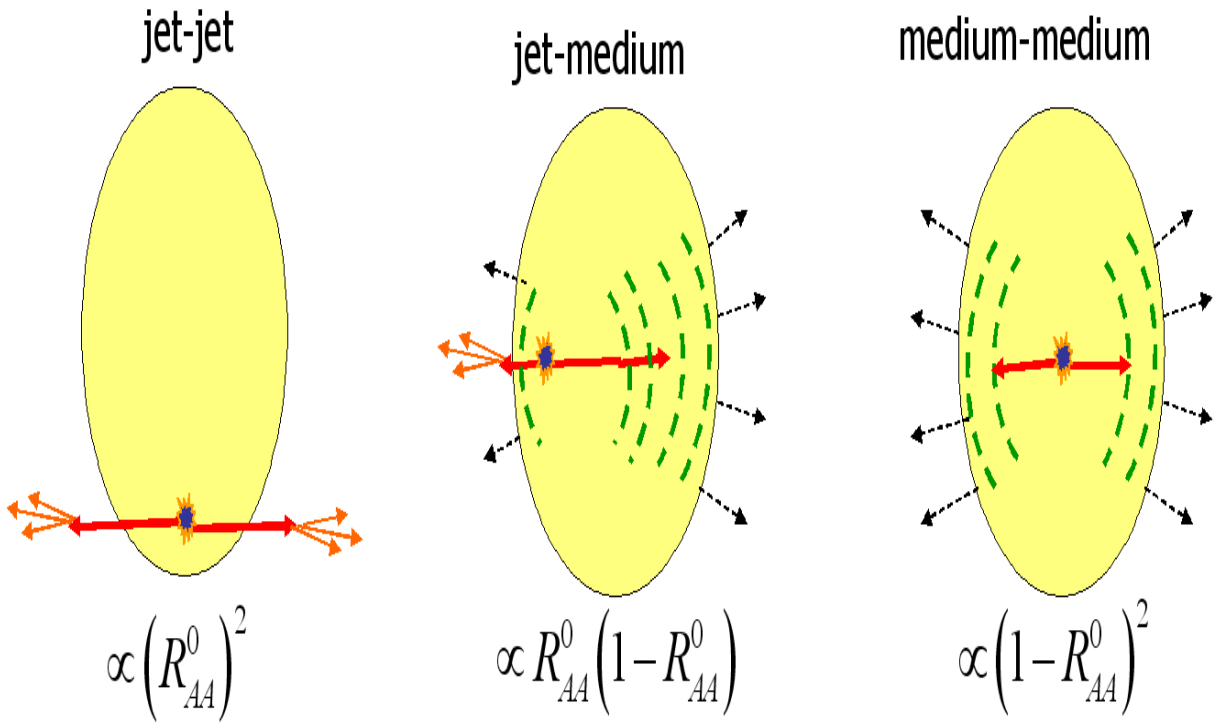

Figure 27: Geometry of jets production in AA collisions at RHIC ($R^0_{AA} \approx 0.2$ is single particle yield suppression factor at large $p_\perp$ in central AA collision) (from arXiv:0805.0160 by Jiangyong Jia).

The nuclear modification factor

$$R_{AA}(p_\perp) = \frac{dN(A+A \to h+X)/dp_\perp dy}{< T_{AA} > d\sigma(N+N \to h+X)/dp_\perp dy}$$

where $< T_{AA} >$ is nuclear overlaping function which is the ratio of the number of the binary nucleon-nucleon collisions, $N_{coll} >$, calculated in Glauber model.

• The important RHIC and LHC heavy ion results are the observation of the strong secondary particle suppression and jet quenching coming from the interaction of the energetic quark or gluon with Quark-Gluon Matter.

• Perturbative contribution (radiative and elastic) is rather small and need to introduce very dense gluon matter to produce sufficient suppression. Additional problem is to describe a large heavy quark jet quenching.

• In spite of the fact that density of produced QGP at LHC ($dN_g/dy \approx 2000 - 4000$ in Pb-Pb collision at $\sqrt{s_{NN}} = 2.76$ GeV)is about factor twice larger than at RHIC ($dN_g/dy \approx 1000 - 1400$ for Au-Au collision at $\sqrt{s_{NN}} = 200$ GeV) experiments at LHC show that the nuclear modification factor is approximately the same as at RHIC. Furthermore,

for heavy quarks it is about $R_{AA}^{c/b} \approx 0.5$ at $p_\perp > 3$ GeV at LHC in comparison with $R_{AA}^{c/b} \approx 0.2 - 0.3$ at RHIC.
See recent paper by Horowitz and Gyulassy Nucl.Phys. **A872** (2011) 265 "The surprising transparent sQGP at LHC"

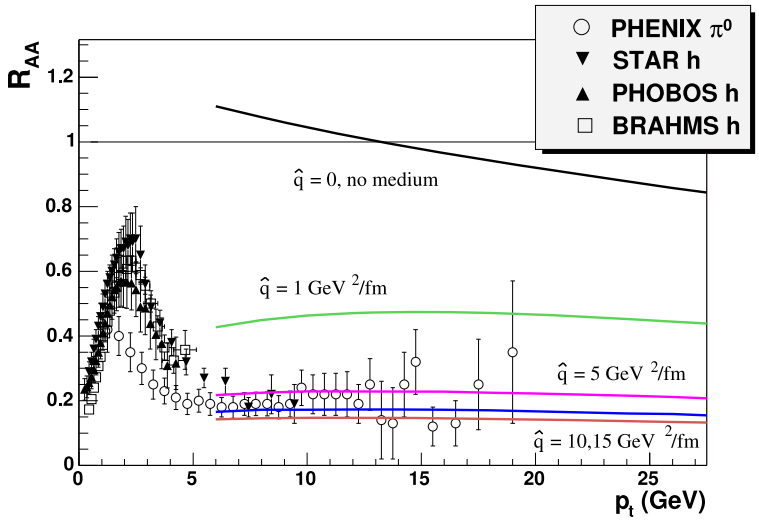

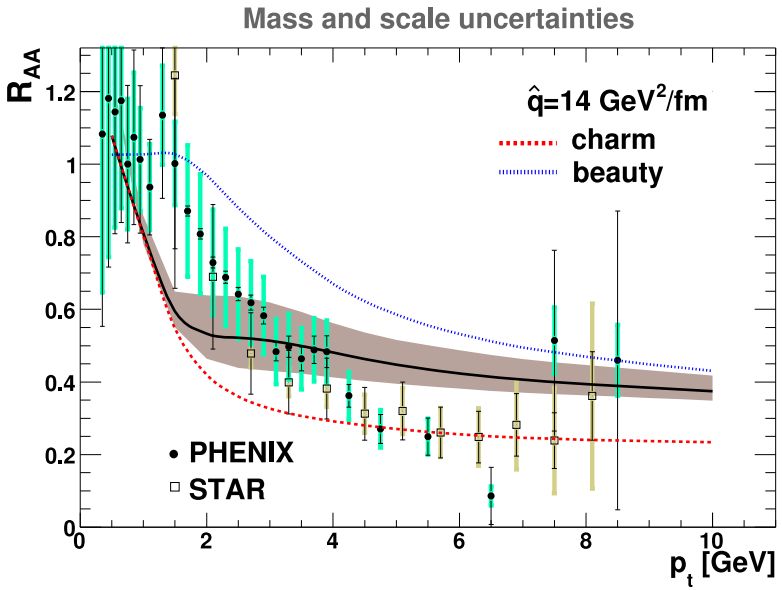

Figure 28: Left: Nuclear modification factor, R_{AA}, for light hadrons in central AuAu collisions at RHIC at $\sqrt{s_{NN}} = 200$ GeV in comparison with estimations based on radiative and collisional energy loss (Eskola et al. NP, **A747** (2005) 511). Right: R_{AA} for non-photonic electrons with the corresponding uncertainty from the perturbative benchmark on the relative b/c contribution. Curves have taken the from paper by Salgato NP, **A783** (2007) 225.

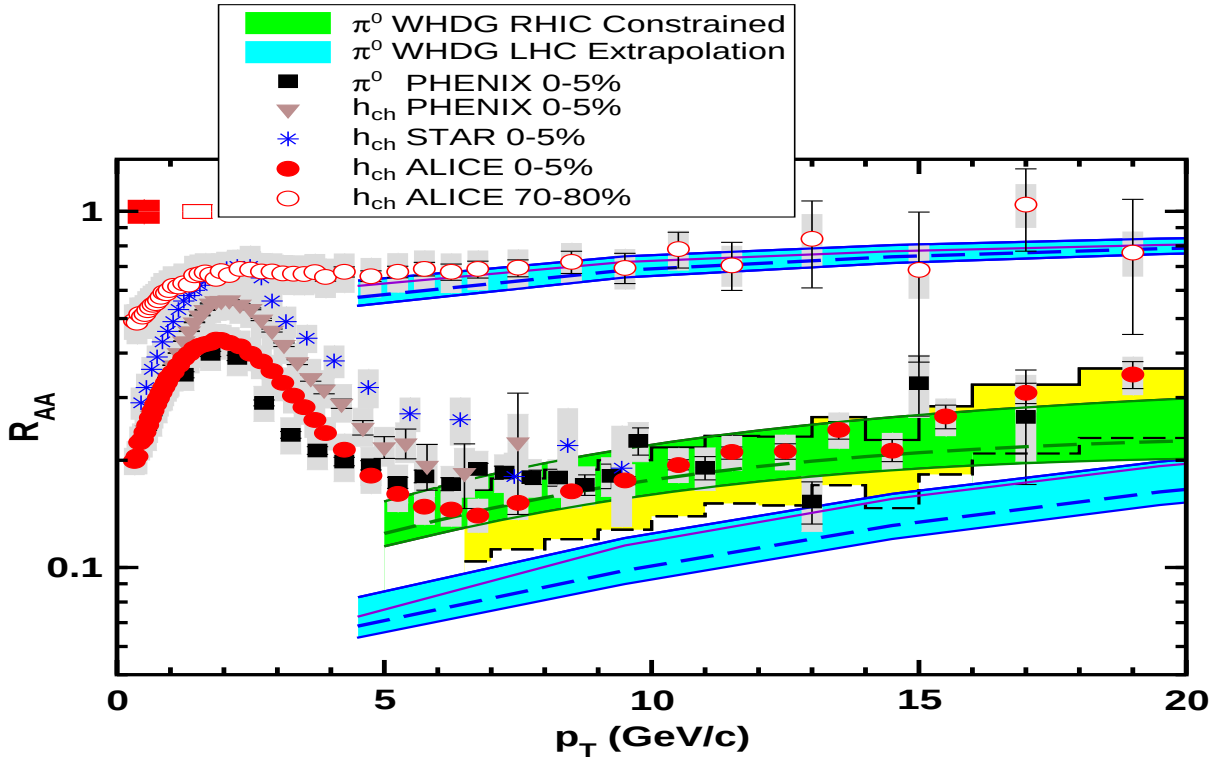

Figure 29: Comparison R_{AA} nuclear modification factors at LHC and RHIC in comparison to Gyulassy et al. WHDG model NP, **A784** (2007) 426.

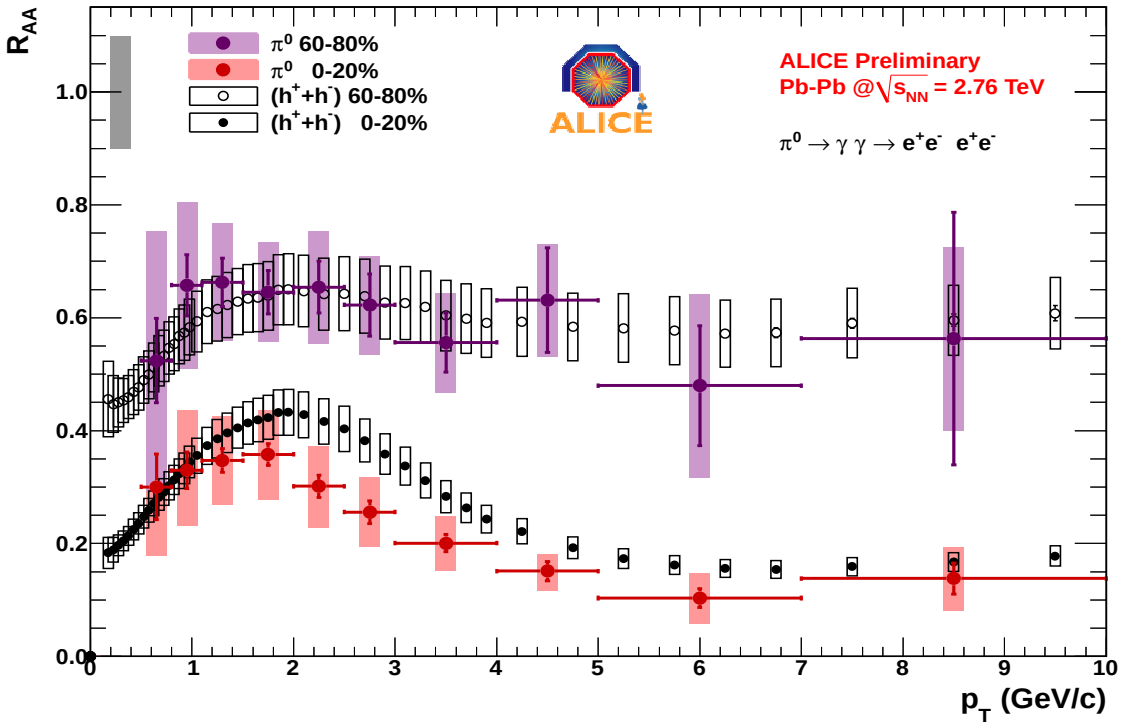

Figure 30: R_{AA} suppression factor at LHC.

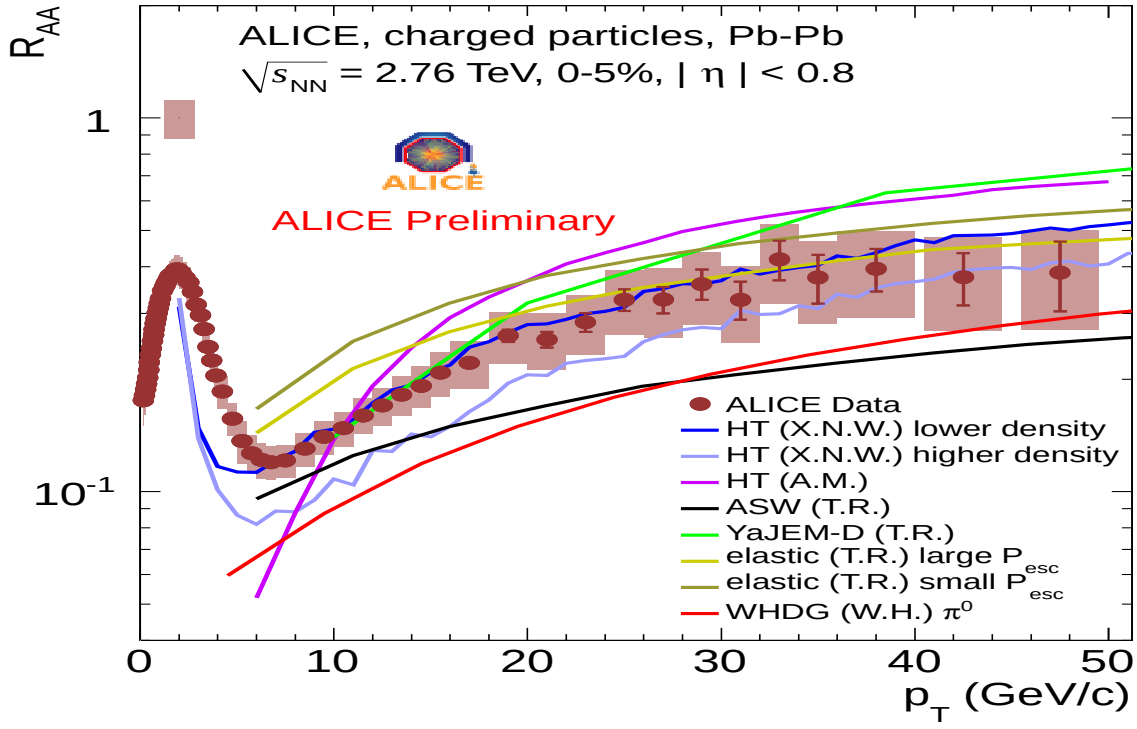

Figure 31: Models for R_{AA} suppression factor at LHC.

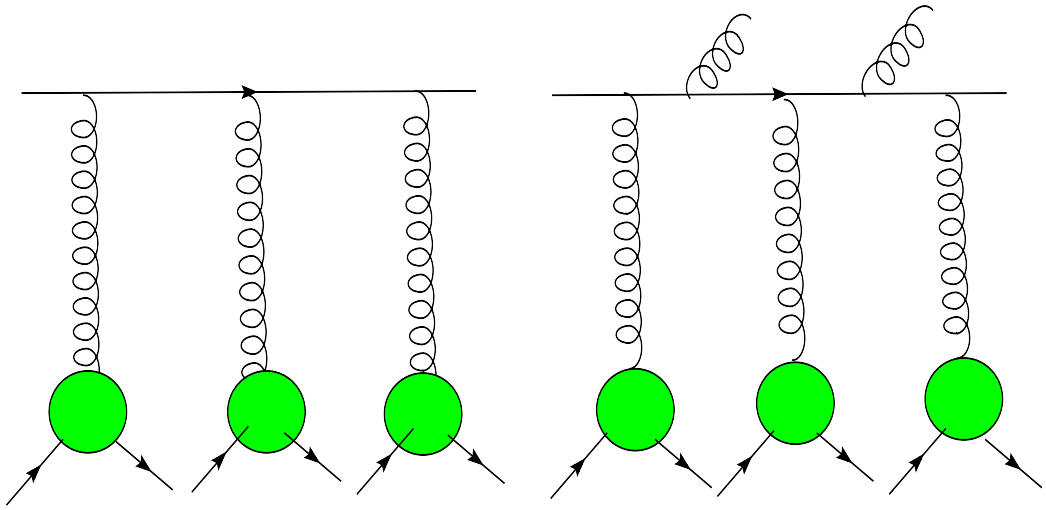

Figure 32: The pQCD a) elastic and b) radiative energy losses.

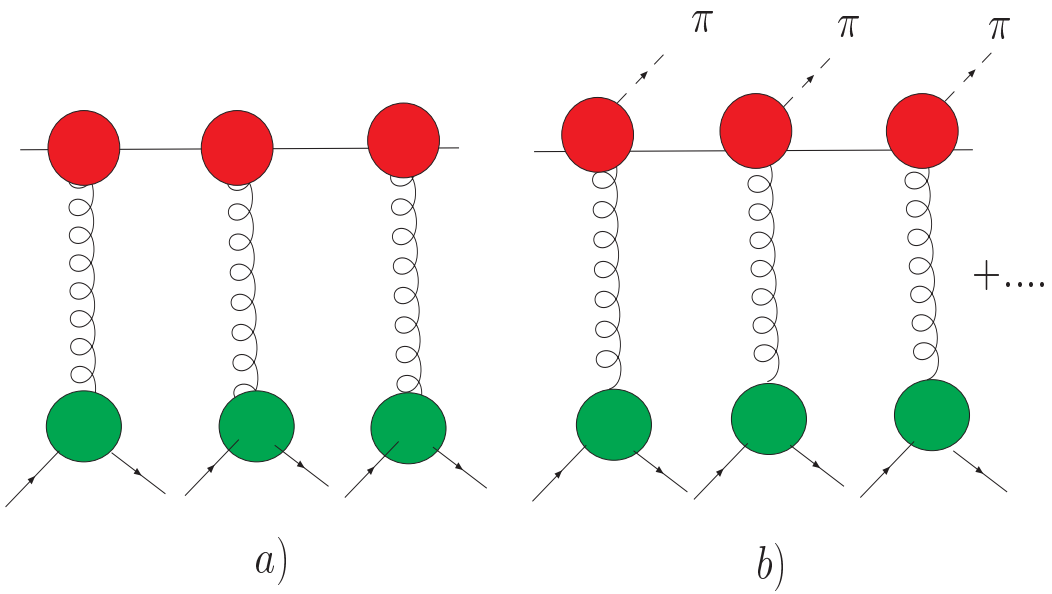

Figure 33: Induced by AQCM non-perturbative a) elastic and b) radiative energy losses.

- **Bjorken's pioner paper (1982)**

Energy loss by energetic partons in hot Quark-Gluon Plasma (elastic (collisional) pQCD energy loss):

$$\frac{dE}{dx} = \int d^3k\rho(k)[Fluxfactor]\int dt\frac{d\sigma^{pQCD}}{dt}(E-E') \sim N_{sc}$$

where gluon and quark densities are given

$$dn_{g,q} = N_{g,q}\frac{d^3k}{(2\pi)^3}(e^{\beta k} \mp 1)^{-1} \equiv \rho_{g,q}d^3k$$

and $\nu = E - E'$ energy loss in single scattering and N_{sc} is the number of scatterings, $N_g = 16$ and $N_q = 12N_F$ and $\beta = 1/T$. The pQCD cross-sections are given

$$\frac{d\sigma_{ij}}{dt} = d_{ij}\frac{2\pi\alpha_s^2}{t^2}$$

with $d_{qq} = 4/9, d_{qg} = 1$ and $d_{gg} = 9/4$. Kinematics: $s = 2kE(1 - cos(\theta))$, $\mid t \mid = s\nu/E$. Flux factor$= (1 - cos(\theta))$ and θ is angle between the incident partons in lab.system.

Bjorken obtained:

$$\frac{E^B_{q,g}}{dx} = \left(\frac{2}{3}\right)^{\pm 1} 2\pi(1+\frac{n_f}{6})\alpha_s^2 T^2 ln\frac{4TE}{\mu},$$

where $\mu \approx m_D$ is Debye screening mass in QGP:
in leading order $m_D^2 = (1+\frac{1}{6})4\pi\alpha_s T^2$.
This formula is relativistic adoption to pQCD case of Bethe-Bloch (1935) formula for ionization energy loss of charged particle in matter.

Transport coefficient for energy loss

$$\hat{q} = \rho \int t \frac{d\sigma}{dt} dt$$

For cold nuclear matter $\rho \approx 0.16$ fm^{-3} and

$$\hat{q}^{pQCD}_{cold} \approx \frac{3\pi^2\alpha_s}{2}\rho[xG(x,Q^2]$$

For small x region $[xG(x)] \approx 1-2$ and we have got (Baier, Dokshitzer,

Mueller et al NP, **B484** (1997) 265.)

$$\hat{q}_{cold}^{pQCD} \approx 0.05 - 0.1 GeV^2/fm$$

For hot QGP at $T \sim 240$ MeV for RHIC (for LHC $T \sim 300$ MeV)

$$\hat{q}_{hot}^{pQCD} \approx 1 GeV^2/fm$$

It is TOO SMALL to explain RHIC data!

In general, the density of QGM decreases strongly in time due to longitudinal and transverse expansion. Averaged transport coefficient

$$\hat{q} = \frac{2}{L^2} \int_{\tau_0}^{\tau_0+L} \tau \hat{q}_\tau(\tau) d\tau$$

• **Two main ingredients in the calculation of energy loss in quark-gluon matter:**

- Density of scattering centers
- Cross section of the parton-medium interaction

The density of scattering centers is usually fixed by effective temperature of QGP which might be related to the average density of gluons and quarks $dN_{g,q}/dy$ created in the AA collision. Such density can be estimated from rapidity density of produced hadrons ($dN_g^{RHIC}/dy \approx 1000$) by using Bjorken model for central high-energy AA collision (see, for example, Wicks et al NP, **A784** (2007) 426). For central Au-Au collision at RHIC at $\sqrt{s} = 200$ GeV , $T \approx 240$MeV ($\approx 2T_c$).
(Definition of rapidity and pseudorapidity:

$$y = \frac{1}{2} ln \left(\frac{E + p_L}{E - p_L} \right), \quad \eta = \frac{1}{2} ln \left(\frac{\mid \vec{p} \mid + p_L}{\mid \vec{p} \mid - p_L} \right).$$

Estimation of R_{AA} in factorization approach

Inclusive particle production cross section

$$d\sigma_{med}{}^{AA \to h+X} = \sum_f d\sigma_{vac}{}^{AA \to f+X} \bigotimes P_f(\Delta E, L, \hat{q}) \bigotimes D^{vac}{}_{f \to h}(z)$$

where P_f is so-called quenching weights (probability to lost amount of energy ΔE, D is the fragmentation function and

$$d\sigma_{vac}{}^{AA\to f+X} = \sum_{ijk} f_{i/A}(x_1, Q^2) \bigotimes f_{j/A}(x_2, Q^2) \bigotimes \hat{\sigma}_{ij\to f+k}.$$

$$d\sigma_{med}{}^{AA\to h+X} \sim \int d(\Delta E) P(\Delta E) \frac{dN^{vac}(p_\perp + \Delta E)}{dp_\perp dy}$$

For example, for exponential partonic cross section $dN/dp_\perp \sim exp(-ap_\perp)$ one finds $p_\perp$-independent nuclear modification factor

$$R_{AA}(p_\perp) \sim \int d(\Delta E) P(\Delta E) exp(-a\Delta E)$$

Non-perturbative energy loss induced by AQCM

In formulas for energy loss the dominated contribution is coming from low $-t$ region.
Therefore the calculation of energy loss should be done within *nonperturbative QCD framework*!

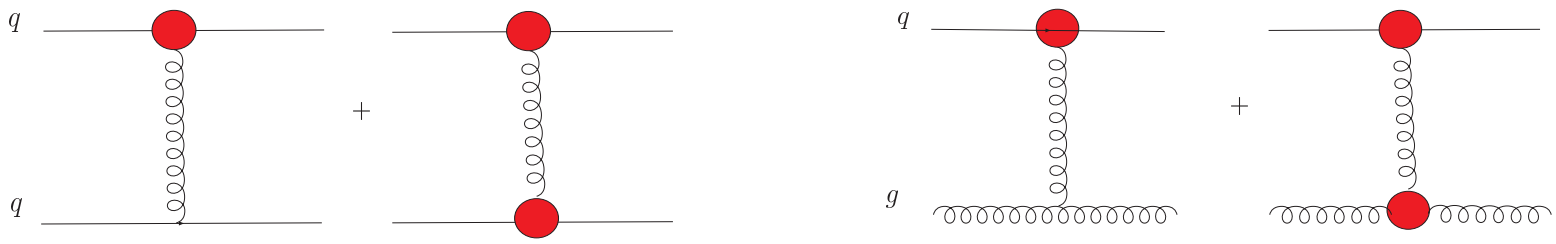

Figure 34: Nonperturbative contribution energy loss by interaction of fast quark with medium quarks (left panel) and with gluons (right panel).

The ratio of the nonperturbative and perturbative collisional energy losses

$$R_{q(q,g)}(E) = \frac{\hat{q}^{nonpert}}{\hat{q}^{pert}} = \frac{\int (d\sigma^{AQCM}/dt)tdt}{\int (d\sigma^{pQCD}/dt)tdt},$$

where in the integral $\mid t \mid_{min} \approx m_D^2(T)$ and $\mid t \mid_{max} \approx ET$. At $T \approx 240$

MeV at RHIC and for $N_F = 3$, Debay mass is $M_D \approx 733$ MeV, for LHC $T \approx 300$ MeV and $M_D \approx 890$ MeV.

We have got for AQCM $\mu_a = -1.$ for RHIC at $E = 10$ GeV $R^{RHIC}{}_{qq} = 3.93, R^{RHIC}{}_{qg} = 2.42$, and for LHC at $E = 60$ GeV $R^{LHC}{}_{qq} = 4.45, R^{LHC}{}_{qg} = 2.62$
If $\mu_a = -1.6$ as for DP value for M_q then $R^{RHIC}{}_{qq} = 7.7, R^{RHIC}{}_{qg} = 3.8$ and $R^{LHC}{}_{qq} = 8.8, R^{LHC}{}_{qg} = 4.2$.

Nonperturbative QCD effects give the dominated contribution to collisional energy loss by fast quark in hot QGP at $T/T_c \approx 1 - 3$!
.

• But, we assumed that density of instantons does not change significantly in interval $T = 0 - 3T_c$!

• Ilgenfritz and Shuryak (1989,1994) shown that instanton density does not change rapidly and above T_c the arrangement of instanton ensemble to so-called "molecular" phase is happen. They introduced "cocktail" model which includes "random" and "molecular" components in instanton liquid.

• **But even if we would only consider "molecular" component above T_c we will still have strong nonperturbative contribution. For example, for RHIC for value of AQCM $\mu_a = -1$ we have $R^{RHIC}{}_{qq} \approx 1.5$ and for $\mu_a = -1.6$ $R^{RHIC}{}_{qq} \approx 4$.**

CONCLUSION

• Instantons induce large anomalous quark-gluon chromomagnetic interaction.

• This interaction provides a new type nonperturbative spin dependent forces between quarks in hadrons. It should be very important in hadron spectroscopy.

• This interaction gives the dominating contribution to the soft Pomeron exchange.

• Internal spin structure of soft and hard Pomerons is different.

• Non-even number of gluon exchanges induced by chromomagnetic interaction leads to the Odderon spin-flip effective exchange

• Anomalous chromomagnetic quark-gluon interaction gives the fundamental nonperturbative QCD mechanism for large single-spin asymmetries observed in many reactions at high energy.

- **AQCM leads to the large partonic energy loss in strongly interacted Quark-Gluon Plasma**